In Vitro Models for Biomechanical Studies of Neural Tissues

Barclay Morrison III, D. Kacy Cullen and Michelle LaPlaca

Abstract In vitro models are invaluable tools for studying cell behavior in a highly controlled setting. Cell and tissue culture models of the nervous system can be utilized to elucidate neurobiological phenomena that are difficult to observe, manipulate, or measure in vivo. In the context of biomechanics, culture models that accurately mimic specific brain features can be used to determine tissue properties and tolerances to mechanical loading. There are several criteria that culture models must meet in order to complement in vivo and macroscopic biomechanical studies. In addition to providing an environment that is conducive to cell survival, cell type and source are critical to the interpretation of results. In this review, we present design criteria for ideal cultures, the current state of the art in neural cell and tissue culturing methods, and the advantages and limitations to using culture mimics. We will further present what insights in vitro models can provide to complement in vivo and macroscopic biomechanics in terms of meso- to microscale material properties and tissue-level tolerance criteria. The discussion will focus primarily on central nervous system (CNS) tissue, which is inherently complex in cytoarchitecture and organization. In addition, the CNS is not typically exposed to mechanical loading beyond physiological motion; therefore, it is expected that cell death and functional failure may be particularly prominent at large deformations and high loading rates. These and other

B. Morrison III (✉)
Biomedical Engineering, Columbia University, 351 Engineering Terrace, MC 8904, 1210 Amsterdam Avenue, New York, NY 10027, USA
e-mail: bm2119@columbia.edu

D. K. Cullen
Neurosurgery, University of Pennsylvania, 105 Hayden Hall, 3320 Smith Walk, Philadelphia, PA 19104, USA

M. LaPlaca
Biomedical Engineering, Georgia Institute of Technology, 313 Ferst Drive, Atlanta, GA 30332-0535, USA

Stud Mechanobiol Tissue Eng Biomater (2011) 3: 247–285
DOI: 10.1007/8415_2011_79
© Springer-Verlag Berlin Heidelberg 2011
Published Online: 30 April 2011

factors must be considered when attempting to extract and culture CNS tissue or its components for studying neurobiological or neuromechanical phenomena.

1 Neural Tissue Structure and Composition

1.1 Heterogeneity of Brain Tissue

Brain is a heterogeneous tissue that is divided into distinct anatomical and functional regions. The gray and white matter comprise the cellular constituents, and the blood supply, cerebrospinal fluid/ventricular system, interstitial fluid, and extracellular matrix (ECM) make up the extracellular components. The intracellular space (ICS) and the extracellular space (ECS) can be considered as one scale of heterogeneity. The ICS is a composite with neurons and their extensions, glia cells, vascular cells, and other support cells. The orientation is quite organized in some areas and apparently random in others. Most neuronal communication in the brain exists on a local level (i.e. shorter interneurons, which comprise most neurons in the brain), with 1,000s of synapses on some neurons, creating an extremely complex network [1]. The brain has a very high cellularity compared to other organs and a very diverse cell population. Cell sizes range from <10 to >100 μm in cell soma diameter with axons ranging from microns to 100s of microns long. Dendrites are highly branched, permitting diversification and maximization of interactions between communicating neurons [1].

Brain tissue can be divided further by anatomical regions. Just rostral to the spinal cord is the brain stem, a deep, well-protected portion of the brain comprised of the medulla oblongata, pons, and midbrain, which houses the controls to many homeostatic functions such as respiratory and cardiovascular regulation. The cerebellum, dorsal to the brainstem, helps control balance, posture, motor coordination, sensory and motor relaying. The diencephalon is the deep region of the brain that contains the thalamus (primary relay for sensory input and motor output) and the hypothalamus (neuroendocrine structure critical for maintaining homeostasis). Traveling toward the brain surface are the white matter tracts, the cerebral nuclei (basal ganglia, hippocampus, amygdala) and the cerebral cortex, comprised of six distinct, organized, interconnected layers. The isolation of any brain region (for primary culture) should consider the connections with other brain areas not represented in the culture and the possible effects (e.g., activation of compensatory responses) harvest and dissection may have. Interneuronal connections and interregional junctions are disrupted during tissue dissociation as are projection axons for most culture techniques, therefore the culturing procedures must consider these microinjuries and provide conditions conducive for repair and healthy culture maturation and reconnection. Some regions, such as the hippocampus are particularly vulnerable to excitotoxicity and the pH of the medium and constituents should allow for normal receptor function and neurotransmitter reuptake. Yet, this region is ideal for studying phenomena related to excitotoxicity, such as ischemia and trauma.

1.2 The Extracellular Space of Brain Tissue

In addition to the cell composition, the ECS is critical for communication, transport, and is essential for normal homeostatic function. It is approximately 20% of the total intracranial volume with half of this volume attributed to the blood and half to the cerebrospinal fluid (CSF) [2]. Some macroscopic parameters used to characterize brain tissue structure are the volume fraction of ECS and effective diffusivity or tortuosity. The ECS is composed of ECM proteins, as well as ions, neurotransmitters, metabolites, and peptides among other molecules. As most cultures are derived from prenatal or perinatal tissue, one must consider that the ECS is larger in the developing brain (36–46% by volume) than the adult, which may play an important role in the diffusion of nutrients and waste. The size of the ECS is especially important, since in most tissue culture systems it is essentially infinite. From a functional point of view, the anisotropy and inhomogeneity of brain tissue dictates the ECS shape, volume, and tortuosity, and hence intraneural (or interneuronal) diffusion parameters. For example, excess neurotransmitters, in addition to cellular reuptake, may diffuse to nearby capillaries or along elongated structures such as white matter tracts [3, 4]. Diffusion of extracellular substances will be discussed below in light of brain tissue dynamics and the artificial culture environment.

2 Neural Culture Models

Cells and tissues of the body may be explanted and kept alive ex vivo for extended periods of time, a process termed cell or tissue culture. Keeping the explanted tissue alive (i.e. metabolically active and functional) and preserving its phenotypic state similar to the in vivo state requires specialized culture conditions and nutrient medium reproducing vital conditions found in vivo. Specialized equipment required includes a tissue culture incubator which maintains physiological temperature (37°C) and gas tension (5% CO_2), laminar flow cabinets to maintain sterility, and in some cases bioreactor perfusion systems as described below. Explanted tissues may be cultured as thin slices of tissue, called organotypic slice cultures, or dissociated into suspensions of single cells to be plated as dissociated cultures. Cultures grown immediately after explantation are referred to as primary cultures.

2.1 Culture Model Utility

Cell and tissue culture models of the nervous system are desirable platforms for studying cell responses to various stimuli, including biochemical and pharmacological investigations, electrophysiological assessment, and mechanical stimulation

or injury. These types of manipulations are not mutually exclusive and therefore it is critical to take into account the multimodal reactions that may follow a seemingly simple input. Well-characterized culture models, therefore, must mimic the cell states of brain tissue, including cell phenotype(s), cell–cell connections, cell-extracellular communication, mechanical properties, chemical composition, and electrochemical balance. The advantages of a well-defined culture preparation are that the complexity of an intact organism is drastically reduced and the culture (both extra- and intracellular environments) can be manipulated much more readily than in an animal or human. Despite the inherent simplicity of culture systems, they can be invaluable for use in understanding neural function as well as supra-physiological states. In order to assemble realistic brain tissue surrogates in a dish, one must rigorously prioritize the above characteristics and properties in a non-biased manner. Simply put: do existing cell and tissue culture models mimic brain tissue? What key parameters are to be mimicked?

2.2 Design Criteria for Brain Mimetics

In order to recapitulate brain tissue in culture models, several criteria are critical and are represented in various degrees of fidelity among culture models. The source of the tissue must be considered in terms of species, developmental age, and brain regions. The type of culture is equally important: primary cells versus cell lines, dissociated cells plated in a constraint-free culture vessel or in a reaggregate or constrained (e.g., scaffold) format, cultured explants or slices (see Table 1). In some instances, a single cell type is desired, yet multi-typic cultures are becoming more commonplace given the complex intercellular interactions that contribute to cellular response. In addition, as discussed above, the immediate extracellular environment must be defined in terms of medium, medium supplements (serum vs. defined supplements), substrate, dimension (2D or 3D), gas composition, pH, and temperature (Table 1).

In addition to these basic design considerations, specialty applications, such as mechanical property testing, mechanical and electrical stimulation, and fluidic control may require further manipulation. Geometric control will preserve the volume fraction of cells to extracellular space and relies on representative cell–cell connections and tissue-like cellular orientation. To this end, slice cultures meet this criterion. Topological features, such as soma shape, neuritic branching and glial-neuronal interactions are often lost with cell dissociation, yet can be maintained through culture manipulation (e.g., scaffolding).

While most brain regions can be cultured, we will focus on hippocampal and cortical dissociated and organotypic cultures in the subsequent sections. The particular purpose of a culture study should consider the cell type(s) to be cultured, as well as the source, age of animal, and other experimental variables. For an

Table 1 Neural culture variables and considerations. Adapted from Ref. [5]

Design Consideration	Culture Options
Cell source/cell type	Rodent fetal and neonatal
Convenience	Cortex, hippocampus, cerebellum, spinal cord, and sensory ganglia are common
Adapted developmental age	
Similarities with human nervous system	
Culture type/culture configuration	Organ, slice, and explant (fragment) cultures
Preservation of anatomy/histiotypic organization	Disaggregated or reaggregated cells and cell lines
Electrophysiological integrity	
Ability to culture from developing & adult animals	
Replicate cultures, cell accessibility, cell subset purification	
Culture Environment	37°C, 100% humidity, 5% CO_2/95% air
Extracellular fluid composition	Culture medium such as DMEM, DMEM/F12, or Neurobasal as neural cells require specific concentrations of ions, amino acids, vitamins, cofactors, hormones, mitogens (for proliferating cells), and other metabolites
Temperature, pH, gas phase	
Substrate	
Dimension	
	Additional supplements include fetal bovine or horse serum, or chemically defined supplements

exhaustive methods-based description of culture methods across the regions of the nervous systems, the reader is referred to [5].

2.3 Dissociated Cell Cultures

Specific cell populations may be isolated from animals or humans and dissociated, or separated from each other, to acquire a suspension consisting of numerous single cells. The classes of dissociated cell cultures consist of primary cells, secondary cells, and/or cell lines, which are then plated in some configuration (see Table 1) based on experimental objectives. Primary cell cultures consist of cells that are isolated directly from tissues and plated for experimentation. Primary cells therefore may closely represent the endogenous phenotype; however, many primary neural cell types are difficult to keep alive for extended periods of time. Secondary cell cultures consist of cells that were permitted to proliferate for several cycles in vitro prior to experimental use. This process is referred to as "passaging", and is typically done to amplify the cell number or purify a particular cell population; however, absent genetic manipulation passaging is limited by a finite number of cell divisions (Hayflick principle) [6]. Cell lines are primary cells that have been "immortalized", typically by genetic mutations or insertions, and may represent a clone of a particular type of cell, which can, in theory, be kept in

culture indefinitely. As cell lines may essentially be cultured indefinitely, there is typically an abundant supply with uniform/consistent behavior and ease of experimental manipulation (e.g., transfection). However, issues exist with "clonal variation", and cell behaviors may not always be representative of a population of cells in the body (i.e. discrepancies between primary cells and cell lines of the same lineage) [7].

Dissociated neural cells may be plated on planar (2D) surfaces, on or within three-dimensional (3D) matrices, or formed into 3D spheres, referred to as reaggregate cultures. These general configurations present a spectrum of critical factors that profoundly influence neural cell growth and function, such as culture architecture (2D vs. 3D; affecting morphology/cytoarchitecture), ECM constituents (affecting cell survival and process extension), and cell density (affecting degree of cell–cell interactions). Additionally, these factors are interrelated; for example the three-dimensionality, ECM properties, and cell density affect the ICS-ECS ratio as well as mass transport requirements (see below).

Planar cultures consist of dissociated neural cells plated directly on a rigid substrate, typically polystyrene or glass, with surface modifications to alter charge or present bioadhesive ligands to facilitate cell attachment [8–10]. Also, 3D neural cell cultures have been developed from dissociated cells as reaggregated sphere cultures [11, 12] or by distribution throughout a matrix [13–17]. For many neurobiological questions, the choice of a planar versus 3D culture configuration offers trade-offs between experimental complexity and fidelity in representing a specific response. In particular, important differences exist between cells cultured in planar versus 3D configurations in terms of the distribution and types of cell–cell/cell–matrix interactions, access to soluble factors, and cell morphology that may drastically affect critical neural cell responses [18]. Cells within a 3D bioactive matrix present different types, quantities, and distribution of cell–cell and cell–matrix interactions [19–22] compared to 2D counterparts. Specifically, cells in 3D contact ECM and experience cell–cell interactions (e.g., receptor-mediated, synaptic junctions) in all spatial directions. Alternatively, cells in 2D typically have a majority of the cell surface directly exposed to media, and may only experience cell–cell interactions in a single plane and are exposed to a much larger ECS as compared to the intact tissue organization. Also, the presence of a 3D matrix alters the cellular microenvironment, affecting concentrations of trophic and signaling factors secreted by cells. Not surprisingly, cells cultured in 2D have shown altered responses to exogenous factors independent of changes in surface area [23]. In addition, cells grown in 3D versus 2D environments have a starkly different morphology and cytoskeletal structure [24]. In the case of neurons, somata and growth cones in 2D are flatter compared to cells in 3D which present a rounder, more bulbous shape [25]. Thus, inherent differences in cell–cell/cell–matrix interactions coupled with corresponding alterations in cell morphology and alterations in the cellular microenvironment may have an impact on intracellular signaling and gene expression.

Given that all neural cells in vivo interact within a 3D environment at relatively high cell densities, quasi-planar neural cell culture models have been developed

consisting of dissociated primary cells above a 3D matrix material [26–28]. These systems effectively approximate a 3D morphology/orientation and may support high 2D cell densities. However, cell–cell and cell–matrix interactions are still somewhat constrained, as cells are not distributed throughout the full thickness of the matrix. Conversely, complete three-dimensionality is achieved in reaggregate neural cultures that are developed by rotation-induced reassociation [11, 12, 29]. These systems produce spheres at high 3D cell densities where diffusion-based mass transport is enhanced by convection due to circulating media. In reaggregate culture systems, the volume available for growth is inherently limited based on surface area to volume ratios that permit survival, thus limiting the scope of 3D interactions. Moreover, the ECM components and cellular distribution are difficult to control in reaggregate cultures; however, these models are extremely useful for studying cell–cell interactions, growth, and function at cell densities that closely match those found in vivo. Three-dimensional cell culture models consisting of neural cells distributed throughout a matrix have also been developed [13, 15–17, 30–32]. In these systems, trade-offs exist between culture thickness (i.e., surface area to volume ratio), and hence the scope of 3D spatial interactions, and cell density, necessitating that relatively thick (>500 μm) cultures use cell densities at least an order of magnitude lower than that found in brain cortices [32, 33]. However, using these 3D scaffold-based neural cultures, key parameters governing neuronal survival and neurite outgrowth based on scaffold physical/biological properties and mass transport phenomena have been uncovered. For example, primary dorsal root ganglion (DRG) neurons survive and extend neurites through hydrogel matrices dependent on the (1) physical properties (e.g., agarose pore size [34], stiffness [25]), (2) ligand concentration (e.g., collagen [35], RGD peptides in fibrin [36]), and (3) substrate geometry [37]. Also, in 3D matrices, DRG neurite growth was inhibited by both certain biochemical and mechanical transitions [38], whereas outgrowth was enhanced in engineered matrices by the presence of specific peptide sequences [39]. The survival of primary neurons from the cerebral cortex has been demonstrated within 3D matrices of collagen and/or various hydrogels (e.g., poly[N-(2-hydroxypropyl)-methacrylamide] [16], poly(acrylate) [13], agarose mixed with collagen [15], collagen covalently linked to agarose [32], and Matrigel [31]), In general, primary cortical neuronal survival and the extent of neurite outgrowth are improved by the addition of specific bioactive cell–matrix interactions [13, 15, 16, 32]. However, neuronal survival and neurite outgrowth in 3D matrices are influenced by intrinsic (e.g., neuronal maturation, receptor expression) as well as extrinsic (e.g., matrix mechanical properties, ligand concentration) signals. Complex, non-linear, and often synergistic relationships exist between matrix mechanical properties and the presence and density of a specific ligand. However, these culture systems present a broad scope of 3D cell–cell/cell–matrix interactions, over a length-scale of millimeters. Importantly, these systems may be engineered from the bottom-up, presenting exquisite control over neural cell populations and scaffold parameters to enable optimization based on the individual neural cell populations and cell densities.

Additionally, neural culture models consisting of multiple cell types closer approximate the heterogeneity of in vivo neural tissue. This heterogeneity in cell-type composition may be particularly important to represent such interactions as physical support and metabolic coupling between neurons and glial cells [40–42]. Co-cultures consisting of neurons and glia are typically 2D models, although multi-cellular 3D reaggregate cultures [43, 44] and 3D neuronal-astrocytic co-cultures [14, 45] have been developed. In 2D neuronal-astrocytic co-cultures, the cells typically self-organize into a base layer of astrocytes with neurons on top [46]. Although this distribution spatially constrains neuron-astrocyte and neuron-neuron interactions, planar co-cultures have established a pivotal role for astrocytes in neuronal survival and synapse formation [47, 48]. These neural cell culture models consisting of multiple cell types are capable of maintaining many positive aspects of in vitro modeling while closer approximating additional aspects of neural cytoarchitecture.

2.4 The Effects of Cell Density on Neuronal Survival in 3D Culture

A direct relationship between neuronal plating density and neuronal survival has been found [32, 49]. Primary cerebral cortical neurons were plated in thick (500–600 μm) bioactive matrices at cell densities varying over an order of magnitude (1,250–12,500 cells/mm^3), and culture viability was assessed at 2 and 7 days post-plating. At 2 days, neuronal survival was high in lower density cultures $<$5,000 cells/mm^3, but poor in the higher density cultures. However, by 7 days, there was a parabolic relationship between cell plating density and cell viability, as cultures plated at either lower densities $\leq$2,500 cells/mm^3 or higher densities $\geq$6,250 cells/mm^3 exhibited extremely poor viability ($<$50% for each). However, neuronal cultures plated at 3,750–5,000 cells/mm^3 produced an optimum viability of $\sim$90%. It was postulated that neuronal death in low cell density 3D culture reflected some minimum threshold for neuron-neuron interactions, both physical and chemical, and was likely independent of mass transport limitations. However, mass transport limitations were likely the predominant reason that 3D neuronal cultures exhibited poor viability at high cell densities ($\geq$6,250 cells/mm^3). Taken together, these observations suggest an important balance between diffusional requirements (affecting the higher density cultures) and a potential threshold for cell–cell interactions (affecting the low density cultures). Increasing the cell density in 3D effectively decreases the available space for diffusion, increases tortuosity factors, and increases the overall rates of nutrient consumption and waste production, creating system-specific relationships between culture thickness, cross-sectional area for diffusion, cell type and cell density. Overall, viability in 3D neuronal cultures was highly dependent on cell density, but an optimized cell density range (3,750–5,000 cells/mm^3 for 500–600 μm thick cultures) yielded

cultures with extensive neurite arborization, robust neuronal survival and active outgrowth.

2.5 Theoretical Analysis of Diffusional Parameters

Cell–cell and cell–matrix interactions are important for the reconstitution of brain tissue properties in a culture environment. The cell density is often an important parameter considered for dissociated cultures, directly related to the intercellular spacing, and thus crucial to function. The brain has low porosity and diffusivity compared to many other tissues. This is due, in part, to a high cell density and the tortuosity. Tortuosity is a measure of hindrance due to cellular obstructions to molecular diffusion. The volume fraction of the tissue (α = volume of ECS/volume of tissue) and the tortuosity (λ) have an inverse relationship. The volume fraction is therefore a function of the relative amounts of extracellular space, pore space, and void fractions [50], and is relatively low in brain tissue. For sufficient mass transport, the brain overcomes low diffusivity by maintaining tightly coupled neuronal-glial interactions, with astrocytes in particular having an extension in direct contact with the vasculature. In addition, as with most tissue in the body, a dense vasculature network leaves brain cells in close proximity to a capillary, thus maintaining relatively short distances (typically $<$100 μm) to the convective nutrient source.

However, simple 3D neural cell cultures have no such vasculature, and therefore typically rely on passive diffusion, which alters the cellular microenvironment by driving nutrients in and waste products out. Thus, mass transport phenomena become crucial in affecting the health and viability of neural cells cultured in 3D. Fick's 2nd Law of Diffusion provides a mathematical framework to describe passive diffusion in 3D neural constructs and, in particular, assess the effects of increased cell density. For simplicity, this analysis was performed in one-dimension (e.g., 3D cell culture adhered to a substrate), approximating the cell-containing matrix as a disc (with specified cross-sectional area and thickness in the z direction), and initially assuming a constant diffusion coefficient, D.

$$\frac{\partial C}{\partial t} = D\frac{\partial^2 C}{\partial z^2} \tag{1}$$

This relationship accounts for passive diffusion into the matrix; however, the cells within the cultures are not passive, therefore the rate at which a particular nutrient is consumed must be considered. For this purpose, consumption includes a given nutrient being metabolized or immobilized on or within a cell, which if this process proceeds rapidly, local equilibrium may be assumed to exist between the extracellular (free) and consumed components of the nutrient. In this case, the concentration S of consumed substance is assumed to be first order and will

be proportional to the concentration C of free (diffusing) nutrient by a consumption rate constant, k, described by the relationship $S = kC$. This consumption rate constant will be specific to a particular compound, as some nutrients freely cross the cell membrane while others exhibit specific mechanisms of entry. Also, consumption will vary as a function of cell number, cell type and level of metabolic activity. Accordingly, Fick's 2nd Law may be modified to become

$$\frac{\partial C}{\partial t} = D\frac{\partial^2 C}{\partial z^2} - \frac{\partial S}{\partial t} = D_c\frac{\partial^2 C}{\partial z^2}, \text{ where } D_c = \frac{D}{k+1} \tag{2}$$

where a new diffusion coefficient, D_c, is the diffusion coefficient given nutrient consumption, and is a synthesis of the free diffusion coefficient and the consumption rate constant. Assuming a large nutrient source (i.e. bulk medium volume above the matrix), the resulting concentration profile, $C(z, t)$, within the cell culture may be calculated. The mass entering the matrix may then be described by the integration of the concentration profile times the effective area for diffusion (A_{eff}) over the thickness (w) through the matrix:

$$M = \int_0^w C(z,t)A_{eff}dz \tag{3}$$

In acellular constructs, A_{eff} would be equal to the overall cross-sectional area of the matrices; however, in cell-containing matrices, A_{eff} is the total cross-sectional area of the matrix minus the average area (per plane) occupied by cells:

$$A_{eff} = A_{total} - A_{cells} \tag{4}$$

Thus, mass transport in this system is (1) governed by the diffusion/consumption characteristics of a particular compound, (2) proportional to the effective cross-sectional area for diffusion, and (3) effectively delayed by the culture thickness. For this analysis, the effective area for diffusion may be considered inversely proportional to cell density, as the open porosity of the matrix was assumed to be constant and thus not affected by cell density. Changes in diffusional area are demonstrated in confocal reconstructions of 3D neuronal cultures plated at various cell densities [49]. Increases in cell density will increase the tortuosity of the system as an enhanced cell-neurite network necessitates increasingly convoluted pathways for diffusion. Although this analysis addressed the rate of nutrient consumption, this relationship may be modified to describe the rate of metabolic waste production and subsequent diffusion out of the cellular microenvironment. This process will also be adversely affected by increases in cell density as this will increase the rate of waste production, possibly creating an unhealthy microenvironment for the cells. Here also, increases in culture thickness will serve to delay clearance of the waste from deep within 3D constructs.

Overall, mass transport must surpass specific metabolic thresholds for 3D culture systems to support viable cells, and given the inter-relationship between

cell density (determining the effective area for diffusion) and culture thickness, changes in one parameter may compensate for another provided mass transport thresholds remain surpassed. In particular, the mathematical analysis was a useful tool to demonstrate that increasing the cell density in 3D effectively hinders mass transport by decreasing the available area for diffusion, increasing tortuosity, and increasing the rates of nutrient consumption and waste production. This analysis supports our conclusion that mass transport limitations were the predominant reason that 3D neuronal cultures exhibited poor viability at high cell densities ($\geq$6,250 cells/mm^3) [51]. Indeed, it has been demonstrated that enhanced mass transport through forced interstitial convection through the 3D neural cell cultures using custom-built micro-bioreactors was sufficient to support neuronal and neuronal-astrocytic co-cultures at cell densities of 10,000–50,000 cells/mm^3 (depending on total culture volume) [32, 33]. Thus, using interstitial convection to enhance mass transport enabled the construction of thick neural constructs approaching the cell densities of 100,000–1,000,000 cells/mm^3 reported in various cortical regions in vivo [52, 53].

Thus, there are important design considerations and limitations that must be acknowledged for 3D in vitro systems. Although our analysis focused on the effects of cell density and culture thickness in relatively large volume cultures ($\sim$200 μL), it is important to note that these factors alone will not dictate mass transport thresholds. To be complete, the overall construct dimensions, geometry, and physical properties need to be taken into account (e.g., surface area to volume ratio, thickness, pore size, tortuosity, etc.). For instance, reaggregate cultures (or neurospheres) may have a cell density of 1,000,000 cells/mm^3, which at several hundred microns in diameter have a high surface area to volume ratio potentially sufficient for support via passive diffusion (although there are necrotic cores in many cases). In non-optimized 3D cultures, cells may experience diffusional transport limitations, causing essential nutrients to be absent from some cells and possibly leading to accumulation of toxic waste products. Such phenomena may have devastating effects on cell survival, or insidiously may confound experimental results by altering gene expression, detrimentally effecting protein production and fidelity, and leading to appreciable deviations from in vivo behavior [54]. However, properly designed and optimized 3D models, where diffusional limits are not approached, may more faithfully recapitulate elements of native tissue than 2D models.

2.6 Application of 3D Neural Cell Cultures

Neural cell culture models have been reconstituted in 3D constructs to study neural mechanobiological phenomena within 3D microenvironments [14, 17, 31, 32, 45]. These models consisted of either predominantly primary cortical neurons or separately isolated primary cortical neurons and cortical astrocytes, each harvested from rodents, dissociated using standard techniques, and mixed in controlled ratios

[14, 31, 32]. These neural cells were homogeneously distributed throughout the full thickness of bioactive scaffolds (typically 500–600 μm thick, up to 1 mm in some cases), and were maintained using a defined, serum-free, Neurobasal medium. Various ECM- or hydrogel-based scaffolds, including Matrigel (i.e., laminin, collagen IV, entactin, heparan sulfate proteoglycan [55, 56]), collagen IV, and/or agarose have been used. Notably, these systems may be engineered from the bottom-up, with precise control over cellular (e.g., phenotypes, ratios, densities) and scaffold parameters (controlling mechanical properties and extent of bioactive motifs), to assess the influences of specific cellular and environmental factors on mechanobiological responses.

Neural cell survival, neurite growth, and functional maturation within these constructs were characterized. At the initial time of 3D plating, the dissociated neural cells had a spherical morphology (absent neurites) and were entrapped throughout the thickness of the matrix. Over days in culture, there was considerable process outgrowth resulting in the formation of 3D, interconnected neural networks by one week [31, 32]. Plating density was a critical parameter for neurons in 3D, with an optimal cell viability obtained at 3,750 cells/mm^3 (based on the starting surface area to volume ratio) [49]. Astrocytic presence significantly improved long-term culture viability, as cell viability in neuronal cultures was $\sim$90% at 7 days, but <70% at 21 days, whereas viability in co-cultures was >95% up to 21 days. Notably, long-term survival of 3D neuronal-astrocytic co-cultures was observed out to over 60 days in culture (unpublished observation).

Moreover, neuronal maturation was demonstrated through the expression of mature isoforms of neuron-specific cytoskeletal proteins and proper electrophysiological function over weeks in culture [45]. The presence of astrocytes also enhanced expression of neuronal functional markers via an increased rate of synapse formation and increased number of synapses per neuron. Neurons in 3D co-culture were found to have normal resting membrane potentials (average $-$56 mV), expressed voltage-sensitive ion channels (Na^+ and K^+ currents), displayed both spontaneous and evoked action potentials (average spike height 70 mV), and exhibited functional synapse formation and network properties. These tissue engineered 3D neural cell cultures provide an innovative platform for neurophysiological and mechanobiological investigations, and serve as an important step in the development of more physiologically-relevant neural tissue models.

2.7 Organotypic Slice Cultures

An alternative to artificial constructs, slices of brain tissue can be cultured for extended periods of time (i.e. in excess of 1 week) given the appropriate environment, thereby allowing the tissue to recover from the trauma of dissection. These cultures are surprisingly stable, maintaining the in vivo anatomy with high fidelity. Organotypic cultures are typically produced from young animals (<P11), and efforts have characterized the in vitro maturation process in detail, suggesting

that they mature in vitro, albeit at a slower pace than in vivo. These culture systems represent an in vitro substrate between the complexity of in vivo models and simplicity of dissociated cell culture, and have been used in models of mechanical injury [57, 58]. Cultured structures include hippocampus [57–59], cortex [60], thalamo-cortical slices [61], whole coronal brain sections [62], and transverse sections of the spinal cord [63, 64].

A critical determinant of organotypic culture health is gas transport which has been addressed through a number of strategies. In one method, tissue was adhered within a plasma clot to a cover-slip placed in rotating tubes with medium [65]. Cultures were sequentially submerged in medium and exposed to the atmosphere ensuring adequate gas exchange and nutrient supply. One limitation was that the cultures thinned to one or two cell layers thick [65–67]. An alternative strategy which produced much thicker cultures many cell layers thick maintained cultures on a silicone membrane with gentle rocking [57, 62]. A third method maintained thick cultures atop a porous membrane with medium delivered through the pores [68–70].

Slice culturing has been observed to begin with an initial period of degeneration which was mostly cleared away by 5 days in vitro (DIV) [69, 71]. Over time, the total number of cells remained constant with only a 12% decrease at 21 DIV [69]. Neuronal numbers remained constant over 21 DIV in the thicker interface cultures [69]. Since total protein content remained constant, the thinning of the interface cultures may be explained by compaction of the ECS which is reminiscent of developmental compaction in vivo [69, 70].

At the single cell and ultrastructural levels, some initial modifications due to the harvesting procedure were noted, but after about a week, cells and synapses developed normally [69, 71–74]. As early as 4 DIV, synaptic density began to recover [65, 69, 71], and by 28 DIV synaptic density was similar to age-matched in vivo levels [69, 72]. The neuronal projections of CA1 and CA3 were fairly resistant to remodeling, although some occurred [67].

Microtubule associated protein-2 (MAP2), a cytoskeletal component, isoform expression (protein and message) mirrored the in vivo developmental program [75, 76]. Tau, another cytoskeletal protein, was initially expressed as a single isoform, but by 14 DIV, four isoforms were expressed, a process not replicated in dissociated cultures [75, 76]. Myelin basic protein (86%) and NCAM (neural cell adhesion molecule) isoforms (71–80%) were expressed at close to adult levels [76]. After an initial drop, MK-801 and AMPA binding, indicative of functional glutamate receptor expression, recovered by 5–10 DIV to in vivo levels [76, 77]. Glutamate receptor subtypes GluR1, Glur2/3, and NMDAR1 were expressed at comparable levels to age-matched controls (50, 40, and 43%, respectively), although GluR4 was aberrantly expressed [76]. The anatomical pattern of excitotoxic death was similar to the in vivo pattern suggesting an anatomically correct distribution of NMDA, AMPA, and kainate receptors [78, 79].

Within the slices, the DG to CA3 to CA1 excitatory pathway was well preserved, although with some sprouting [80]. Over the first weeks in vitro, field population spike and excitatory post-synaptic potential (EPSP) amplitudes

increased until approximately 28 DIV and then stabilized [72, 81, 82]. Induction of long term potentiation (LTP), a cellular correlate of learning, was possible after 9–15 DIV, whereas in vivo, LTP can be induced after post-natal day 14 (P14) [72, 81]. Paired pulse facilitation (PPF), a measure of short-term synaptic potentiation, emerged in culture at approximately the same time as in vivo [72, 81]. Cultures grown on cover-slips were more excitable than interface cultures, possibly because of the substantial thinning and loss of cells, potentially including inhibitory interneurons [83, 84]. In contrast, thicker cultures were less excitable and did not burst when followed out to 80 DIV [70, 85].

Progress has been made in the long-term culture of hippocampal tissue from either P20 [86] or as old as P30 [85] rat pups, although long-term culture of fully adult hippocampal tissue is not currently possible [87]. Greater success has been achieved with transverse spinal cord cultures which can be produced from mice as old as P21–42 [63].

3 Neural Mechanical Properties

Existing experimental data and scaling relationships have been used to empirically derive mechanical thresholds to predict physiological outcome in animal experiments [88]. In order to examine cell and tissue level responses, high resolution finite element models (FEMs) require material properties on a corresponding scale. It is imperative that these assigned material properties coincide with those of living tissue to ensure accurate predictions of mechanical response to stress and strain in vivo. In addition to providing increased fidelity to FEMs, the material properties of living tissue can be emulated in culture systems that study mechanical cellular response.

3.1 Mechanical Properties of Brain

Measuring material properties of the brain poses particular challenges, in part due to its high cellularity as detailed above. Without the proper environmental conditions, e.g. adequate gas exchange, nutrient medium, hydration, correct osmolarity, temperature, and pH, cells within the excised tissue will die rapidly altering mechanical properties of the tissue. Determining mechanical properties under the same conditions required for culturing brain tissue avoids many of these pitfalls which may have confounded earlier investigations. A large range of shear moduli have been reported for different species, times postmortem, preconditioning, and frequencies/times, but a consensus is emerging that the shear modulus of brain is around 1 kPa, increasing with rate or frequency [89, 90].

Brain is one of the softest tissues in the body. Therefore to measure reaction forces during testing requires either very sensitive transducers or large

samples. Previous studies using relatively large samples (10–30 mm) have used shear [91–95], compression [96, 97], or tension [98, 99]. See in Chapter "Brain Tissue Mechanical Properties" of this volume for detailed discussions of brain properties at macroscopic scales. The use of relatively large tissue samples (at least 10–30 mm) makes the production of a homogeneous tissue sample difficult (depending on the structure of interest and species), thereby complicating interpretation of results. Brain is structurally heterogeneous with gray and white matter at the grossest level of distinction with many finer features (on the order of microns and millimeters) apparent upon histological examination. The use of smaller samples allows measurement of material properties of sub-regions and smaller structures and is aided by the use of novel, highly sensitive microprobes.

One motivation to measure material properties of anatomical structures in the brain is that inclusion of heterogeneous material properties in computational models affects the induced strain fields and hence the pattern of tissue injury [100]. Only by inclusion of particular anatomical structures within a model can the predicted injury pattern be compared and validated against the in vivo histological injury pattern. For example, the CA3 pyramidal layer of the hippocampus is particularly vulnerable to fluid percussion injury (FPI) models of TBI [101]. Predicting this preferential cell loss in CA3 with a computational model would be a substantial step toward its validation.

An alternate testing methodology that is less constrained by sample size is indentation [102–106]. Anatomical regions of interest can be tested in situ, limited by the size of the indenter and the sensitivity of the force transducer. Recently, this approach was used to measure linear viscoelastic mechanical properties of anatomical structures within coronal sections of the rat brain through stress relaxation experiments with a flat circular probe of radius 250 μm [106]. The CA1 subfield of the hippocampus was the stiffest brain region tested, whereas other hippocampal regions (CA3 and dentate gyrus) were significantly softer. The cerebellum was the most compliant region of the brain tested. On average, white matter regions were softer than gray matter, and about a two-fold difference between the stiffest and most compliant brain regions was observed (Fig. 1). Overall, the brain became stiffer with animal age.

To capture the time-dependent relaxation behavior, multiple linear viscoelastic constitutive models were fit to the data, including a Prony series approximation (Eq. 5), a continuous phase lag model (Eq. 6) [107, 108], and a power law model (Eq. 7) [109].

$$G(t) = G_{\infty} + \sum_{j} G_j \cdot \mathrm{e}^{-\frac{t}{\tau_j}} \tag{5}$$

$$G(t) = G_{\text{inst}} \left[\frac{1 + c\left[\int_{\tau_2}^{\tau_1} \frac{e^{\frac{-1}{x}}}{x} dx\right]}{1 + c \ln\left[\frac{\tau_2}{\tau_1}\right]} \right] \tag{6}$$

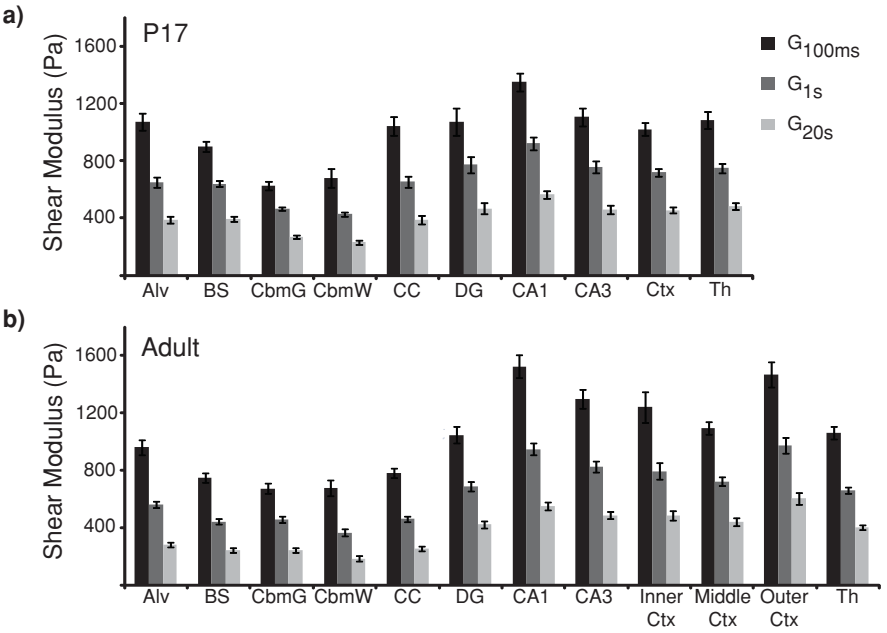

Fig. 1 Time dependent shear modulus determined from stress relaxation indentation experiments is presented for brain tissue of different aged rats: **a** P17 and **b** adult. Modulus is presented at specific time points during the relaxation after indentations of approximately 10% strain (mean ± standard error of the mean). Overall, adult brain was slightly stiffer. White matter was softer than gray; the cerebellum was the most compliant structure tested. *Alv* alveus, *BS* brain stem, *CbmG* cerebellar gray matter, *CbmW* cerebellar white matter, *CC* corpus callosum, *DG* dentate gyrus, *CA1* CA1 region of the hippocampus, *CA3* CA3 region of the hippocampus, *Ctx* cortex, *Th* thalamus. Reproduced with permission from Mary Ann Liebert [106]

$$G(t) = \frac{k}{\Gamma(1-\beta)} t^{-\beta}; k = \frac{A}{\tau^{-\beta}} \tag{7}$$

The Prony series fit the complete data set with the largest R^2 value, although all model fits were greater than 0.92. Although the Prony series fit yields a non-unique set of parameters, its implementation into FEMs is straightforward, since it is usually an included constitutive description.

The main limitation of the indentation methodology is that the strain field beneath the indenter is not uniform. For a flat circular indenter, strains are maximal at the indenter edge consisting of both compressive and tensile strains. An analytical solution for calculating shear modulus exists:

$$G(t) = \frac{1}{4} \cdot \frac{P(t)(1-v)}{R\delta} \tag{8}$$

in which P is the reaction force, R is the indenter radius, δ is the indentation depth, and v is Poisson's ratio [110, 111]. The analysis assumes the tissue is homogeneous, isotropic, an infinite half-space, and that linear elasticity applies (i.e. small strains). A hereditary integral can be used to determine $G(t)$ if δ is not an ideal step function. Deviations from the analytical solution are influenced by the ratio of indenter radius to specimen thickness [112]. Additionally, although our study utilized a small indenter ($R = 250$ μm), the probe was a similar size to some of the anatomical structures of interest. Actuator vibration and force transducer sensitivity limited the use of smaller probes and faster indentation rates.

To further improve the spatial resolution of testing methods, the atomic force microscope (AFM) has been adapted for indentation of living brain tissue or brain cells [104, 105, 113]. With nano-Newton force resolution and micron spatial resolution, the AFM is well-suited for mechanical testing of brain allowing the use of micron scaled probes. Using a spherical tip of radius 12.5 μm so as to measure tissue properties as opposed to sub-cellular properties, significant differences were found between different anatomical structures within the hippocampus [104, 105]. For example, the CA1 pyramidal layer which contains neuronal cell bodies was the stiffest structure in the adult brain [105]. It was significantly stiffer than the adjacent CA1 stratum radiatum which is comprised of neuronal processes and glia. Another region within the hippocampus, the dentate gyrus was only 25% as stiff as the CA1 pyramidal layer in the adult brain at an indentation depth of 3 μm (approximately 30% indentation strain). These differences may be large enough to affect the induced strain field caused by injurious loading, thereby strongly influences the pattern of traumatic cell death. Future computational models of TBI may need to include this level of spatial detail to accurately predict regional cell death.

A further complication for characterizing the mechanical properties of brain tissue is its non-linearity with respect to strain. For indentation depths greater than 0.5 μm with a spherical probe of radius 12.5 μm in AFM studies, brain tissue became stiffer with indentation depth [105]. Several other studies using larger samples have reported strain stiffening for brain [95, 114, 115], while others have reported strain softening but usually for lower strains than those analyzed in the AFM study [93, 98]. To capture this non-linear behavior, AFM data was fit to several non-linear elastic constitutive models including Neo Hookean (Eq. 9] [116], Mooney Rivlin (Eq. 10) [117, 118], or Ogden (Eq. 11) [119]:

$$W = \frac{E}{2}(I_1 - 3) \tag{9}$$

$$W = \frac{C_1}{2}(I_1 - 3) - \frac{C_2}{2}(I_2 - 3) \tag{10}$$

$$W = \frac{2\mu}{\alpha^2}(\lambda_1^\alpha + \lambda_2^\alpha + \lambda_3^\alpha - 3) \tag{11}$$

in which W was the strain energy density, I_1 and I_2 were the first and second invariants of the strain tensor, λ_1, λ_2, and λ_3, were stretch ratios in the principle directions, and E, C_1, C_2, μ, and α were material parameters. The Ogden material description fit the material non-linearity with the smallest mean square error.

Brain mechanical properties were also shown to be age dependent [105]. The brains of younger rats were softer and more homogeneous than adult rats. The increased stiffness correlated with increased lipid content and decreased water content. The effect of age is an active debate as results from another group indicated that younger brain was stiffer [120, 121]. Nonetheless, these results suggest that the induced strain field for younger animals will differ from that of older animals. Such age-dependence may be relevant for designing age-appropriate safety systems for the prevention of TBI.

Because the AFM methodology is inherently an indentation approach, analysis of force deflection curves suffer from the same limitations as described above for the flat circular punch indentation. An added complication for a spherical probe is that contact radius is not constant during indentation. Analytical solutions for spherical indenters exist but make several simplifying assumptions including sample homogeneity, isotropy, infinite thickness, and small strains. The classic solution makes an additional assumption that, for small indentation, the spherical indenter profile can be approximated as a paraboloid. Contact radius was assumed to be $a = \sqrt{R\delta}$ (R and δ defined above) to provide an expression for shear modulus [110]:

$$G(t) = \frac{3}{8} \cdot \frac{P(t)(1-v)}{\sqrt{R\delta^3}} \tag{12}$$

A solution for an explicitly spherical indenter also exists, but is slightly more complex as the expression for contact radius is transcendental and cannot be inverted [122, 123]:

$$\delta = \frac{1}{2} \cdot a \cdot \ln\left[\frac{R+a}{R-a}\right] \tag{13}$$

$$G(t) = \frac{p(t)(1-v)}{\left[(a^2+R^2) \cdot \ln\left(\frac{R+a}{R-a}\right) - 2aR\right]} \tag{14}$$

Note that Ref. [124] contains an error and is missing a 2 in front of the aR term.

The AFM approach can be extended to the viscoelastic regime by applying a small sinusoidal oscillation to the probe tip and measuring the phase difference between the scanner displacement and the probe deflection. Taking the Taylor series expansion of the analytical solution for indentation with a spherical probe for an oscillatory input yields [125–127]:

$$f^*_{\text{osc}} = 4\sqrt{R\delta_\circ}\frac{G}{1-v}\tilde{\delta}^* \tag{15}$$

in which f^{*}_{osc}, the AFM probe force, and $\tilde{\delta}^{*}$, the tissue indentation, are complex quantities with magnitude and phase. Splitting this into real and imaginary components yields the storage (G′) and loss (G″) modulus:

$$G' = \frac{(1-v)}{4\sqrt{R\delta_{\circ}}} \cdot \frac{a_d k a_r \cos\varphi - k a^2}{a_d^2 - 2a_d a_r \cos\varphi + a_r^2}$$
$$G'' = -\frac{(1-v)}{4\sqrt{R\delta_{\circ}}} \cdot \left[\frac{a_d k a_r \sin\varphi}{a_d^2 - 2a_d a_r \cos\varphi + a_r^2} - \omega \cdot \gamma \right] \tag{16}$$

in which δ_0 is the static indentation depth, k is the cantilever stiffness, a_d is the magnitude of the scanner displacement, a_r is the magnitude of the cantilever deflection, φ is the phase lag between the two, γ is the drag of the probe in the fluid, and ω is the oscillation frequency. This methodology has been applied to measure viscoelastic properties of brain, producing both frequency and indentation-depth dependent storage and loss moduli (Fig. 2, unpublished observations). One of the recurring challenges is accurate contact point identification.

Mechanical properties of single brain cells have been measured with a similar approach [113]. Hippocampal neurons and astrocytes were indented with a 3 μm sphere with superimposed oscillations of 30, 100, and 200 Hz, although no indentation depth was reported. Neurons were stiffer than astrocytes. Shear modulus increased with frequency and ranged from about 100–300 Pa.

Several sources of non linear behavior can complicate analysis of dynamic indentation data. The first is the effect of large deformation on material response. If data from large-deformation indentation experiments is analyzed with linear elastic theory, a linearly elastic material will appear non-linear, exhibiting strain hardening behavior [128]. Simple shear excitation does not suffer the same complication. The second is due to the intrinsic non-linear material properties of the tissue which arises as the excitation strain is increased above the linear limit. A third source of non-linearity in response to a single frequency excitation is the existence of higher order harmonics in the tissue response. These higher order harmonics violate the basic assumptions of linear frequency analysis. Several strategies have been described to analyze this non-linear material behavior [129–131]. A Fourier transform of the tissue response will quickly identify whether higher order harmonics are contaminating the data.

3.2 Mechanical Properties of 3D Neural Cultures

In light of what is known about brain tissue properties, rheological properties (specifically, complex modulus) of Matrigel (7.5 mg/mL), a commonly used 3D cell scaffold, were measured over days in vitro as a function of frequency for the

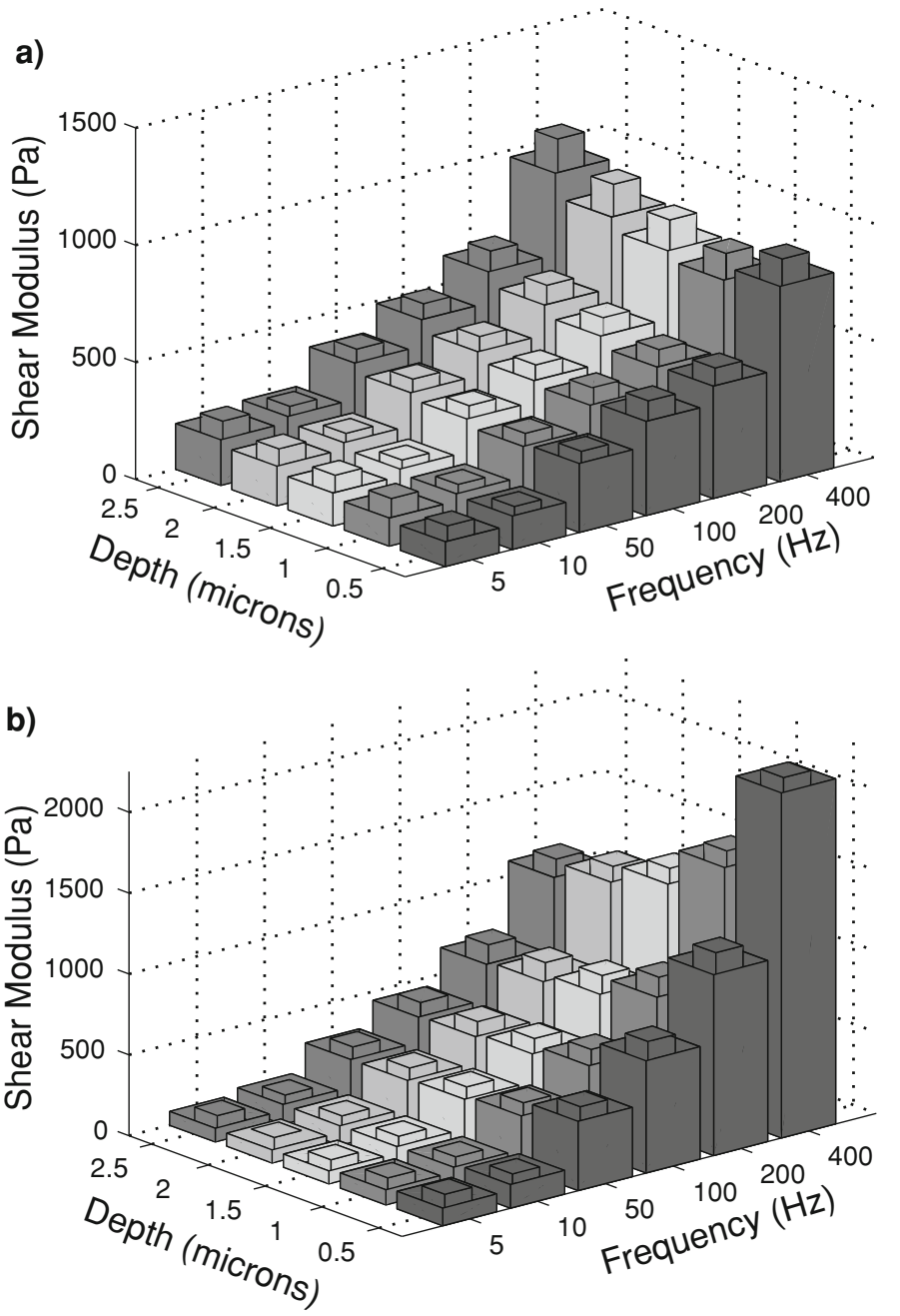

Fig. 2 Depth- and frequency-dependent **a** storage and **b** loss modulus determined from dynamic AFM indentation of the pig alveus with a spherical probe (mean + standard error of the mean). Modulus increased with excitation frequency, consistent with a viscoelastic material. Storage modulus increased with indentation depth, suggesting non-linear behavior

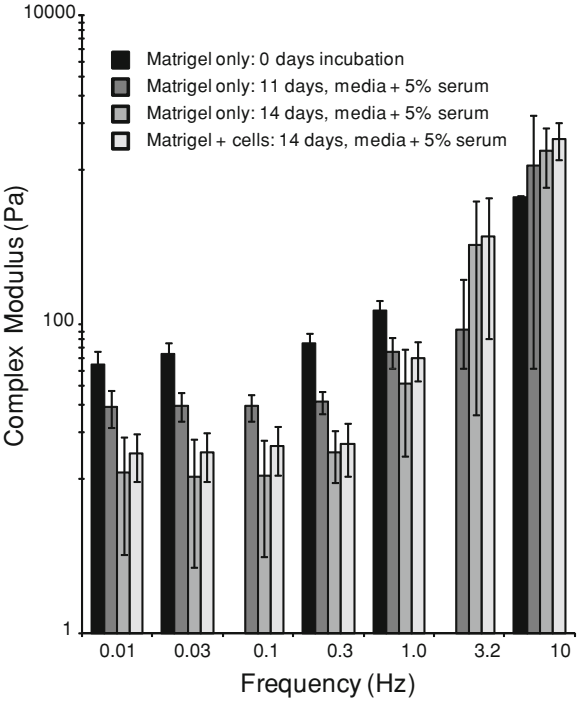

Fig. 3 The complex modulus of thick (500 μm) Matrigel constructs was examined as a function of incubation days, the presence of serum, and the presence of cortical neurons/astrocytes. All dimensions and incubation/rheology conditions were constant for the experimental groups ($n = 2$–4 samples per condition) for a frequency sweep of 0.01–10 Hz. As expected, complex modulus increased with frequency. The presence of serum during gelation and incubation time periods did not affect the baseline properties (i.e. those at 0 days with no serum). Furthermore, the presence of cells did not significantly affect the overall material properties of the 3D culture after 14 days in culture. Data presented as mean ± standard error of the mean

following conditions and time points: (1) Matrigel alone at 0 (immediately upon gelation), 11, and 14 days following casting in serum free cell culture medium at 37°C and 5% CO_2; (2) Matrigel with neurons and astrocytes at 2,500 cells/mm^3 at 14 days in culture at 37°C and 5% CO_2. All groups except the 0 days group contained 5% serum. All rheology experiments were performed in hydrated samples on a Bohlin CVO Rheometer (East Brunswick, NJ) at 37°C under 0.005 strain with a frequency sweep from 0.01 to 10 Hz ($n = 2$–4 samples per condition). The trends among the conditions tested were similar across treatment groups with respect to frequency and time under culture conditions, suggesting that 3D cultures of cortical neurons/astrocytes in Matrigel retain the gross mechanical properties over 14 days and that this was independent of the presence of cells (Fig. 3). Furthermore, the mechanical behavior was similar to that of brain [103–106, 121, 132, 133], further supporting the use of 3D cultures and

emphasizing the need for mechanical characterization. Of note was that the protein concentration and cell density used were optimized previously for viability [51]. At 0.01 Hz, the order of the complex modulus was: 0 days without serum >11 days with serum >14 days (with or without cells, both with serum). At 10 Hz, the standard deviations were large, and as such, these results can only be taken as a trend, however, the following was the order of the central tendencies of the complex modulus: 0 days without serum <11 days with serum <14 days with 5% serum <14 days with cells and 5% serum. Further studies can help resolve the effects of the culture conditions on rheological properties, such as scaffold degradation, serum presence, and cell density.

4 Mechanical Loading of Neural Cell and Tissue Models

4.1 Mechanotransduction in Neural Tissues

Cells from different organ systems in the body experience different mechanical stimuli (from physiological to pathophysiological) and have different thresholds for activating biochemical and gene-level responses. The process of mechanical stimulation causing biochemical and molecular changes is termed mechanotransduction. Mechanotransduction, in general, is the biological mechanism by which cells interact with their environment and is comprised of a set of complex and dynamic processes. Transmembrane receptors, such as integrins, attach to ECM proteins such as collagen, fibronectin, and laminin. Adhesion receptors have specificity to the ECM ligand molecule and thereby, use different extracellular cues to direct various cell behaviors, such as migration and neurite outgrowth. This process involves an intracellular domain that binds to the cytoskeleton and intracellular signaling molecules such as vinculin, talin, paxillin, focal adhesion kinase (FAK), and proline-rich tyrosine kinase 2 (PYK2). While the function of neural adhesion receptors has been well studied under physiological conditions, the role of these receptors in pathologic mechanotransduction remains elusive.

Cells of the CNS are not normally exposed to large deformations and as such, the mechanisms of signal transduction in response to mechanical stimuli in neurons, in general, are poorly understood. Notable exceptions are in the areas of sensory transduction and neural development. Sensory cells such as inner ear hair cells, for example, which are specialized mechanosensing cells, contain inherent mechanisms for transducing stretch to electrical activity [134]. The physical surrounding of a cell as it interacts with other cells directly or through cell–matrix interactions has been shown in many studies to influence normal function. For example, neurons grown on ECM coated elastomer could be electrically stimulated by mechanical indentation of the elastomer; furthermore this was shown to be dependent on intact ECM-cytoskeletal connections [135].

4.2 Mechanical Response of Neural Cultures

Mechanotransduction has been studied in vitro by controlling the mechanical properties (i.e. rigidity, tortuosity, ligand density) of extracellular matrices and observing cell behavior [30, 136–139]. It has been shown that neurons tend to support longer neuritic outgrowth on compliant substrates compared to rigid support scaffolds [25, 35, 140, 141], whereas fibroblasts, spread and migrate more readily as rigidity was increased [142, 143]. When primary cortical neurons were cultured in a 3D environment with controlled mechanical properties and laminin density, however, it was observed that the more rigid formulation ($G' = 565$ Pa) supported more neurite extension than a softer ($G' = 175$ Pa) gel, suggesting that the 3D environment may provide additional extracellular cues for supporting neurons (unpublished observation). Of note, the stiffer gel mechanical properties were closer to that of brain compared to the softer culture scaffold [103–106, 121, 132, 133], suggesting that cell specific tissue properties should be emulated when creating culture mimics. This concept of matching in vivo mechanical properties to culture conditions has been supported by other studies as well [140, 144, 145]. The response to mechanical stimulation may also be affected by the degree of differentiation, type and level of stress, cytoarchitectural complexity, and physical environment. Controlled biophysical cell and tissue culture conditions are especially critical in which the mechanical environment can be independently varied and the neural response directly measured.

4.3 Mechanical Injury to Neural Tissue

By applying a range of mechanical stimuli to neural tissue models, one can better understand specific cellular responses (e.g., neurotransmitter release, signaling pathways). Here, we focus on the mechanical responses to injurious physical insults observed in 2D and 3D neural cultures and the organotypic slice culture models. Ultimately, the identification of mechanotransduction mechanisms can best be achieved through a multidisciplinary approach, with a variety of cellular and tissue models, animal and human studies, and computer simulations. Traumatic insults to the brain and spinal cord deform cellular elements. Persistent injury can occur from a single mechanical event and subsequent insults may exacerbate the initial response, suggesting increased sensitivity due to an abnormal state [146].

Cellular models of traumatic injury have been developed that mimic the mechanical parameters associated with large, high rate deformation to cellular elements of the brain. These in vitro injury model paradigms include transection, compression, stretch, and shear. Two-dimensional in vitro cultures are valuable tools for studying penetrating and blunt impact injury [147, 148], as well as stretch injury [149–151]. Both 3D cultures derived from dissociated cells and

brain slices have been used for neural injury studies [17, 152]. The most appropriate injury models, however, may be those that mimic the 3D in vivo configuration and that capture forces experienced during injury in vivo. In vitro models of TBI allow for well-characterized and repeatable injuries, the parameters of which can be controlled independently and precisely. While various studies have examined cellular and tissue levels thresholds to mechanical loading [31, 153–155], the input parameters inherently vary from system to system, pointing to the continuing need to systematically study a range of mechanical stimuli to different culture systems in a comparative and parallel manner. Some general observations have been made across some laboratories. For example, the rate of application of mechanical loading dictates, to some degree, the severity of the injury [57, 60, 154, 156–160], likely due to the viscoelastic response. Strain level, independent of rate, has also been associated with injury severity [31, 57, 60, 160–162]. It is likely that varying loading regimes, input parameters, cell preparations, time points for outcome measures, and other experimental variables play a role in these different responses. In addition, one must consider the nonlinearities that may be part of the injury response and the range of mechanical parameters with respect to the analogous in vivo loading conditions, many of which are difficult to link to specific pathologies.

Experimental models of superthreshold mechanical stimuli must be defined by: (1) the culture composition (including density, extracellular constituents, cell types, and developmental age) and mechanical properties; and (2) the mechanical parameters (e.g., stress, strain, and modality) that mimic the phenomenon being studied. In vitro systems eliminate systemic responses, while maintaining the ability to manipulate and observe cells during and after physical stimulation [57, 163–166]. Cellular and tissue neural models preserve the ability to apply a more controlled mechanical input than in a correlate in vivo environment. Because complexity, such as additional cell types or extracellular stimuli can be added in a controlled fashion, such models play an important role in discerning the mechanical principles that govern physical and functional response and thresholds.

5 Defining Tolerance Criteria for Neural Tissue

5.1 Definition of Failure

Failure is a central theme of our studies on brain tissue and cultures, and our studies have benefited from a definition that is broader than the typical engineering definition of ultimate failure. Mechanical failure may be an adequate definition for load-bearing tissues of the human body like bone and even for soft tissues in the most extreme cases. However, tearing (fracture) of tissue or cells is only one mode of failure, and many others may exist for biological tissues as discussed below.

A fundamental difference between inert engineering materials and biological tissues is that the latter are alive and perform some form of active, physiological function. Therefore, the very concept of failure must be revised. The exact definition may be tissue-specific such as fracture for bone or laceration for skin. However, these definitions may be too insensitive to identify the onset of injury for the brain, i.e. tolerance criteria. For non load-bearing, highly cellularized, living tissues, failure can be defined in myriad ways and may occur far below mechanical failure limits.

5.2 Tolerance Criteria for Living Brain Tissue

Quantification of tolerance criteria for brain has a number of requirements including a living preparation, a means to apply precisely controlled mechanical stimuli, and a mechanism to verify tissue biomechanics. For brain and other highly cellular tissues, cell death may be a widely applicable outcome. This working definition of injury has been applied to determine tissue-level tolerance criteria for cell death in the rat hippocampus and cortex [60, 160]. In these studies, organotypic slice cultures of brain were subjected to controlled mechanical deformation, and the resultant cell death quantified in a region-specific manner over time [57]. An empirical relationship between input mechanical stimuli (tissue strain and strain rate) and cell death was calculated. The goal was to provide these transfer functions for incorporation into FEMs, providing them with the capability to predict biological responses in addition to typical mechanical parameters such as stress and strain.

It was found that cell death was not immediate in response to deformation that was below cellular ultimate failure limits [57, 60, 160]. Instead, cell death increased over 4 days after injury, highlighting a fundamental difference to engineering materials. Both CA3 and CA1 of the hippocampus were the most vulnerable regions to mechanical injury. Dentate gyrus was less vulnerable than other hippocampal regions. Cortex was much less susceptible than the hippocampus as a whole; interestingly, cell death in the cortex increased with increasing strain rate in contrast to hippocampal cell loss which was insensitive to rate. To illustrate, after 0.20 biaxial strain, approximately 35% of cells in CA1 and CA3 died versus 20% in the dentate gyrus and less than 5% in the cortex.

By quantifying both the input mechanical stimulus and the output biological response, it was possible to determine numerical relationships for predicting the time course and magnitude of post-injury cell death (Fig. 4). These three empirical functions (Eq. 17) could be incorporated into FEMs, thereby equipping them with biological predictions to supplement mechanical predictions of stress and strain.

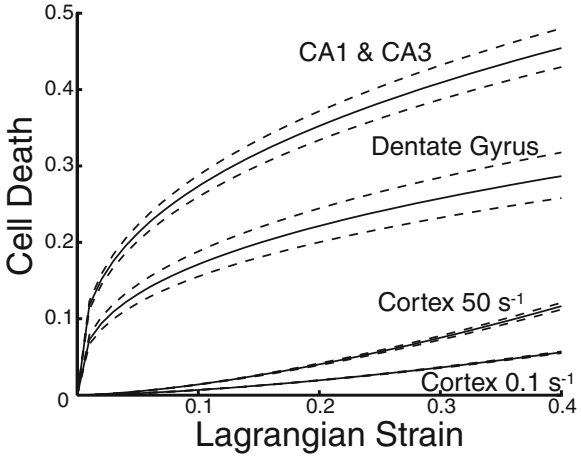

Fig. 4 Mathematical function representing tolerance criteria relating input biaxial strain to resultant cell death 4 days post-injury were derived from experimental data. The *solid line* represents the best fit with 95% confidence intervals indicated with *dashed lines*. The CA1 and CA3 regions of the hippocampus were the most vulnerable, followed by the dentate gyrus. The cortex was much less susceptible. Cortical cell death was dependent on applied strain rate whereas hippocampal cell death was not. Modified with permission from the Stapp Association [60] and with permission from Elsevier [160]

$$\begin{aligned}
\text{CA1\&CA3} &= 0.0389(\pm 0.0011)\cdot \text{Strain}^{0.3663(\pm 0.0029)}\cdot \text{Time}^{2.0150(\pm 0.0216)} \\
\text{DG} &= 0.0323(\pm 0.0017)\cdot \text{Strain}^{0.3721(\pm 0.0056)}\cdot \text{Time}^{1.8209(\pm 0.0407)} \\
\text{Cortex} &= 0.094(\pm 0.0021)\cdot \text{Strain}^{1.5293(\pm 0.0125)}\cdot \text{Time}^{0.8337(\pm 0.0120)}\cdot \text{Rate}^{0.1175(\pm 0.0029)}
\end{aligned} \tag{17}$$

In a similar model of biaxial stretch applied to dissociated cells, neurons from the hippocampus were significantly more vulnerable to injury than were neurons from the cortex (167). Hippocampal neurons died after 30% stretch suggesting a threshold below this level. In contrast, few cortical neurons died after the same mechanical stimulus, suggesting a higher threshold in corroboration of the slice culture findings [60, 160, 167].

An important consideration in modeling mechanobiological responses in neural cells is the complexity of the loading regime. For instance, all cellular strain fields in the brain, whether physiological or traumatic, will be three-dimensional, an inherent consequence of the three-dimensionality of complex neural morphologies and cell–cell/cell-ECM linkages. Moreover, even for relatively homogeneous bulk loading of the head and brain tissue, local cellular strain distributions may be heterogeneous combinations of tensile, compressive, and shear strains. To investigate the effects of strain field complexity on neuronal responses to high strain rate deformation, both 3D neuronal cultures and 2D neuronal cultures (sandwiched between layers of a 3D matrix) were subjected to bulk mechanical loading

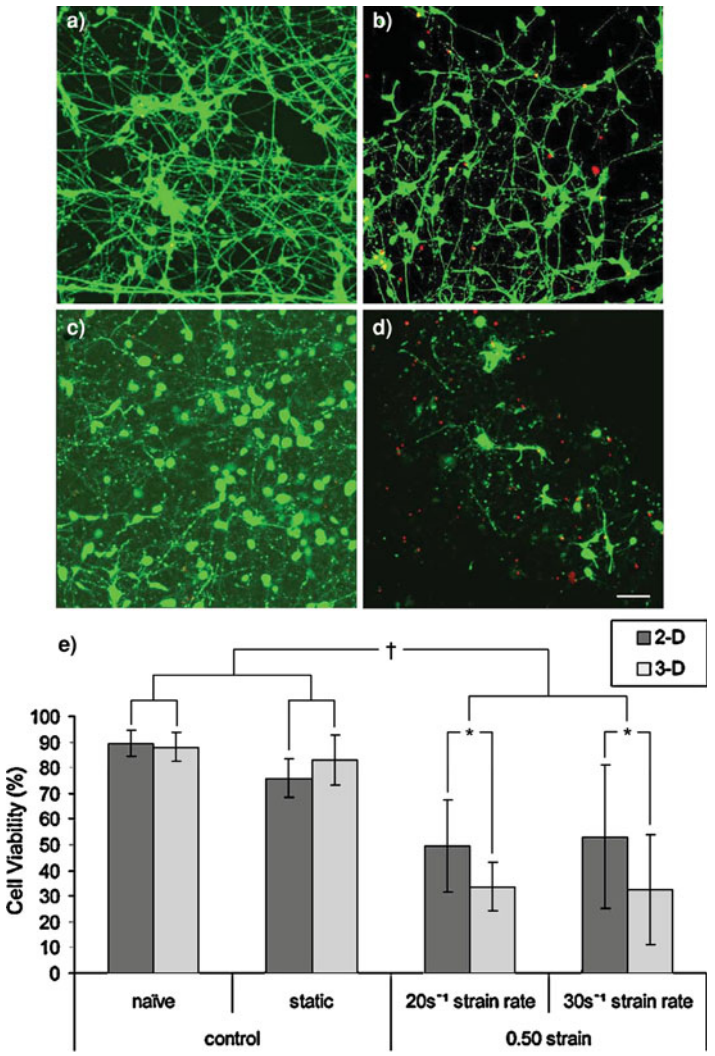

Fig. 5 Cell viability in networks of neurons cultured in 2D and 3D following shear strain. Cells were subjected to high strain rate and magnitude shear deformation using a custom-built device. Viability was assessed 24 h after the application of control or strain conditions (live cells stained in cytosol and appear as larger areas with branching neurite patterns (*green*), nuclei of dead cells stained as punctate smaller areas (*red*)). Confocal reconstructions of neuronal cultures in 2D after **a** static control or **b** 50% strain, $30s^{-1}$ strain rate. Neuronal cultures in 3D after **c** static control or **d** 50% strain, $30s^{-1}$ strain rate (scale bar = 50 μm). **e** Graphical representation of cell viability. There was not a significant difference in viability in naive controls compared to static controls for either 2D or 3D culture; however, there was a significant decrease in both 2D and 3D viability after high rate deformation versus uninjured controls ($\dagger p < 0.05$). Moreover, there was a significant decrease in viability in 3D versus 2D under matched loading conditions ($*p < 0.05$), implicating the complexity of the local cellular strain fields in more detrimental outcome following traumatic loading. Error bars represent standard deviation. Reprinted with permission from Mary Ann Liebert [31]

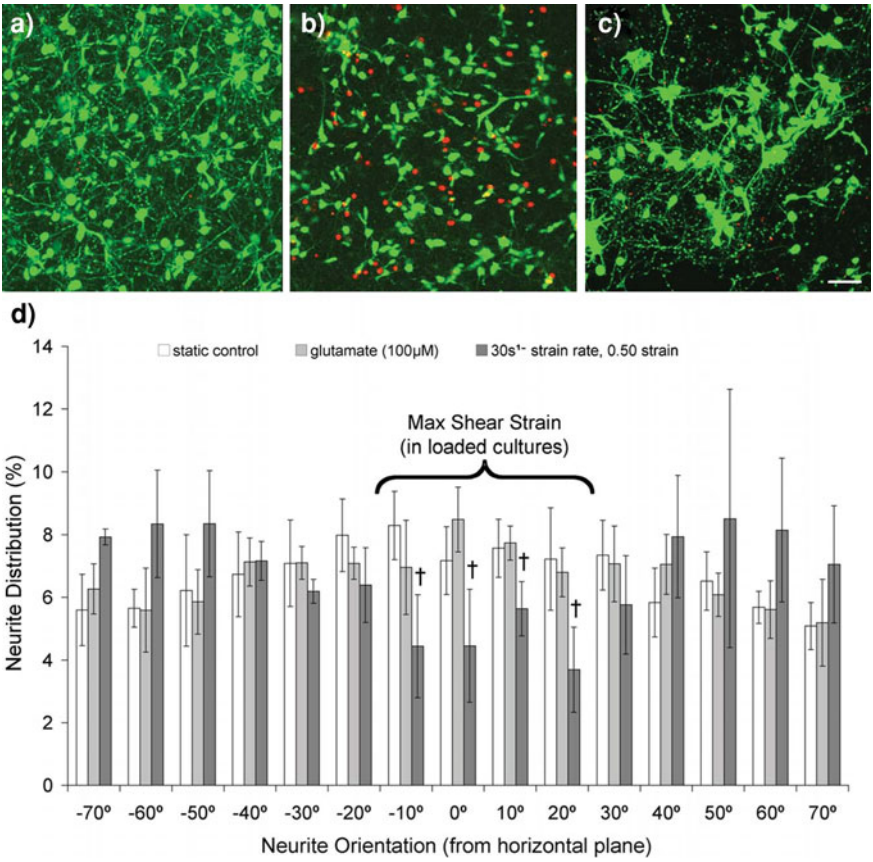

Fig. 6 Neurite loss in 3D neuronal cultures following shear strain. Confocal reconstructions of 3D neuronal cultures at 24 h following **a** sham conditions, **b** excitotoxicity via 100 μM glutamate exposure (positive control), or **c** shear deformation at 50% strain, $30s^{-1}$ strain rate (scale bar = 50 μm). Live neurons and remaining neurites stained with calcein can be seen as rounded structures with typical branching patterns (*green*) and the nuclei of dead cells are seen as punctate bright areas (*red*). There was approximately a 50% reduction in the total number of neurites following either chemical injury (excitotoxicity) or mechanical injury. **d** The orientation of remaining neurites was measured following these conditions. Following excitotoxic injury, the distribution of remaining neurites was consistent across all angles of orientation, indicating indiscriminate neurite loss. However, following high strain rate shear deformation, there was preferential loss of neurites at angles close to the horizontal plane (†$p < 0.05$), correlating with orientations predicted to experience maximum shear strain, suggesting heightened sensitivity to shear strain. Error bars represent standard deviation. Adapted with permission from Elsevier [17]

consistent with tissue-level strains in closed-head TBI [31]. At matched strain magnitude (50% shear strain) and strain rates ($20–30s^{-1}$) to the 3D cell-containing matrices, neuronal death was greater when neurons were cultured in 3D versus monolayer (Fig. 5). These data implicate the complexity of the local cellular strain field, in addition to the magnitude and rate of individual strain components, in

thresholds for neuronal death, and also indicate that tolerances were lower in realistic tissue constructs. Moreover, within these 3D constructs, the unique strain fields of individual neurons and neurites (micro-strains) may be calculated based on the cell orientation with respect to the bulk loading (meso-strains) [17]. This analysis revealed that the majority of neurite loss correlated with the direction of maximum shear strain (Fig. 6), demonstrating increased sensitivity to the strain mode in complex loading regimes.

In comparison to neurons, significant astrocyte cell death was observed after 25% shear strain in the same constructs [17]. Although astrocyte death did not significantly increase after 50% shear compared to 25%, astrocyte death significantly increased as the strain rate was increased from 1 to $30s^{-1}$ [14, 17]. Interestingly, high shear strain (50%), quasi-static ($1s^{-1}$) loading did not induce cell death, although this caused significant astrocyte activation measured by proliferation and hypertrophy, suggesting a direct mechanism of mechano-activation in astrocytes. However, at an intermediate strain rate of $10s^{-1}$ inducing significant cell death, astrocyte activation was maximal [14], demonstrating that local cell death may amplify the astrocyte responses to trauma.

Multiple models injure cultured tissue with uniaxial as opposed to biaxial strains, either by fluid shear [151] or substrate deformation [159]. After fluid shear stress of NT-2 cells, a neuronal cell line, significant lactate dehydrogenase (LDH) release was measured immediately after 16% cell strain and at 24 h after 12% strain at strain rates below $7s^{-1}$ [151, 156]. After uniaxial strain applied to hippocampal cultures by substrate deformation, cell death was significantly increased after 50% but not 17% strain, suggesting a threshold above 17%, although in a follow up study, significant cell death was reported after 6% strain [168, 169]. When hippocampal slice cultures were subjected to uniaxial strain, no activated caspase 3 or calpain was detected after 50% strain. Caspase 3 is essential for execution of the intrinsic apoptotic pathway whereas calpain is activated by elevated intracellular calcium and is thought to play a role in necrotic cell death. Calpain was consistently activated after 75 and 100% uniaxial strain, whereas caspase 3 was activated after 75% but not 100% strain [170]. Although cell death was not directly measured, these results suggest that injury may activate different cell-death pathways depending on severity.

The reasons for the discrepancy in cell-death response after uniaxial loading between the fluid shear stress and substrate strain models may be due to experimental considerations. Verification of cell/tissue deformation was absolutely essential for each experiment. Although tissue may appear to be adhered to the substrate after injury, it may be anchored in only one region such that it does not stretch, but does not float away either. In the shear stress model, cell strain during injury was confirmed, whereas in the uniaxial slice model, it was not.

In a comparison of uniaxial and biaxial strain applied to cortical neurons, the post-injury calcium response was significantly greater after 30 and 50% biaxial strain with very few neurons responding to uniaxial strain [171]. Cell membrane permeability was greater after biaxial deformation, as well [171]. Although no cell

death was measured 24 h after any injury up to 50% strain, these results suggested that biaxial strain may be a more severe injury than uniaxial strain [171].

The brain carries out essential functions of information processing, motor control, and consciousness which are dependent on neuronal electrophysiological function at the cellular level. One can image many injury mechanisms which may alter neuronal function without requiring cell death. Therefore, an additional tolerance criterion may be more appropriate for nervous system tissue: disruption of electrophysiological function. After either 5 or 10% biaxial strain applied to hippocampal slice cultures, evoked activity was significantly altered [172]. The maximal evoked response (R_{max}) was decreased by up to 75%, and the tissue became less excitable with up to 120% increase in the stimulus required to generate a half maximal response (I_{50}) [172]. These studies were conducted with microelectrode arrays (MEA) which have the advantage of sampling tissue activity from up to 60 locations simultaneously, providing unbiased and comprehensive quantification of activity throughout the neuronal network. MEA recordings are also compatible with dissociated cultures. After uniaxial strain via fluid shear stress, acute changes in activity were noted including an increase in burst interval [173].

6 Conclusions and Future directions

Neural cell and tissue culture models offer a unique platform for studying mechanical response to physiological forces as well as neural trauma, where physical forces may cause structural failure due to excessive stress and strain, or result in sublethal dysfunction. Cells in culture, however, may differ in cell–cell configuration, material properties, cell signaling, and gene expression from in vivo counterparts. Recreating these structural components at the nano-, micro-, meso- and macro-scale, together with physiological and physical properties, allows development of robust culture systems, which in turn, aids in developing both constitutive models and guides for computer simulations. The formulation of analytical models that consider multi-scale tissue characteristics then become very powerful tools for assessment of the biomechanical response to various stimuli.

In vitro models of neural cells have proven to be effective in the systematic identification of specific mechanisms of mechanotransduction and injury causation. The primary attributes of in vitro models include control of cellular composition, control of local environment, accessibility for imaging, experimental manipulability, and elimination of systemic effects. In vitro neural models must mimic the in vivo environment in terms of composition, cell type, extracellular space, cell volume fraction, tortuosity, cell cytoarchitecture, distribution of cell–cell/cell–matrix interactions, and the multicellular composition. Properly designed cellular models may serve as a more accurate guide to cellular growth, interaction, and responses to biochemical and/or mechanical stimuli.

In the continued drive to increase the biofidelity of ex vivo constructs to the in vivo brain, new scaffold materials may provide improved substrates to support

higher cell and process density to more closely approximate in vivo brain. Patterning cell types in 3D may allow for replication of the complex connectivity of multiple cell types that typifies the CNS. Our studies have demonstrated the benefits of perfusion for supporting these high cell densities. Microfluidic perfusion systems may hold promise for making these types of cultures more commonplace. Explant culture systems can reproduce a degree of cytoarchitectural complexity in an effort to maintain in vivo characteristics. However, a major limitation is that only post-natal/juvenile tissue can be cultured successfully. Future efforts to culture adult brain tissue would fill a critical need for determining whether tissue-level tolerance criteria are affected by age.

The ex vivo systems provide unfettered access to the cultures at multiple spatial scales. At the tissue level, it has been possible to quantify tissue biomechanics during the applied dynamic event, whether it is injury or mechanical testing. However, dynamic measurement of cellular or subcellular deformation has remained difficult, but could significantly add to our understanding of cell-level biomechanics which may be one source of heterogeneous cellular response. Such insight is essential for multi-scale modeling of TBI with strategies such as representative volume element modeling.

The biological response, as a consequence of mechanotransduction cascades, occurs on a slower time scale than an injurious stimulus. Through the use of fluorescent reporter systems such as optogenetic approaches, continuous monitoring of physiological parameters becomes possible. Correlating the activation of cell death cascades with mechanical injury parameters will further define tolerance criteria and the limits of safe exposures, which are absolutely critical for safety system design.

Analysis of indentation data for the determination of mechanical properties is inherently complex given the heterogeneous strain field beneath the indenter. However, sophisticated numerical analysis methods such as inverse FE approaches could be leveraged to more accurately extract constitutive properties. Such numerical methods explicitly include factors normally ignored in classical indentation solutions. The accuracy of derived constitutive properties is increased by explicitly modeling the complex strain field beneath the indenter, as well. Indentation methods such as these will provide material property data at high spatial resolution, which will be instrumental for the next generation of computation models for simulating TBI and predicting anatomical patterns of cell death. These models, in turn, may be used to design the next generation of safety systems to reduce the socioeconomic costs of TBI.

Acknowledgments The authors thank Varadraj Vernekar, Ph.D. for contributions to the 3D culture mechanical testing study, and Benjamin S. Elkin, Ph.D. for the dynamic AFM indentation studies.

References

1. Kindle, E., Schwartz, J., Jessell, T.: Principles of Neural Science. McGraw-Hill, New York (2000)
2. Sycoma, E., Nicholson, C.: Diffusion in brain extracellular space. Physiol. Rev. **88**, 1277–1340 (2008)
3. Sycoma, E.: Extra synaptic volume transmission and diffusion parameters of the extracellular space. Neuroscience **129**, 861–876 (2004)
4. Sycoma, E.: Diffusion properties of the brain in health and disease. Neurochem. Int. **45**, 453–466 (2004)
5. Fedoroff, S., Richardson, A.: Protocols for Neural Cell Culture, 3rd edn. Humana Press, Totowa (2001)
6. Hayflick, L., Moorhead, P.: The serial cultivation of human diploid cell strains. Exp. Cell Res. **25**, 585–621 (1961)
7. Jacobson, M.: Clonal analysis and cell lineages of the vertebrate central nervous system. Annu. Rev. Neurosci. **8**, 71–102 (1985)
8. Potter, S.M., DeMarse, T.B.: A new approach to neural cell culture for long-term studies. J. Neurosci. Methods **110**, 17–24 (2001)
9. Dichter, M.A.: Rat cortical neurons in cell culture: culture methods, cell morphology, electrophysiology, and synapse formation. Brain. Res. **149**, 279–293 (1978)
10. Corey, J.M., Wheeler, B.C., Brewer, G.J.: Compliance of hippocampal neurons to patterned substrate networks. J. Neurosci. Res. **30**, 300–307 (1991)
11. Choi, H.K., Won, L., Heller, A.: Dopaminergic neurons grown in three-dimensional reaggregate culture for periods of up to one year. J. Neurosci. Methods **46**, 233–244 (1993)
12. Hsiang, J., Heller, A., Hoffmann, P.C., Mobley, W.C., Wainer, B.H.: The effects of nerve growth factor on the development of septal cholinergic neurons in reaggregate cell cultures. Neuroscience **29**, 209–223 (1989)
13. O'Connor, S.M., Andreadis, J.D., Shaffer, K.M., Ma, W., Pancrazio, J.J., Stenger, D.A.: Immobilization of neural cells in three-dimensional matrices for biosensor applications. Biosens. Bioelectron. **14**, 871–881 (2000)
14. Cullen, D.K., Simon, C.M., LaPlaca, M.C.: Strain rate-dependent induction of reactive astrogliosis and cell death in three-dimensional neuronal-astrocytic co-cultures. Brain Res. **1158**, 103–115 (2007)
15. O'Connor, S.M., Stenger, D.A., Shaffer, K.M., Ma, W.: Survival and neurite outgrowth of rat cortical neurons in three-dimensional agarose and collagen gel matrices. Neurosci. Lett. **304**, 189–193 (2001)
16. Woerly, S., Plant, G.W., Harvey, A.R.: Cultured rat neuronal and glial cells entrapped within hydrogel polymer matrices: a potential tool for neural tissue replacement. Neurosci. Lett. **205**, 197–201 (1996)
17. LaPlaca, M.C., Cullen, D.K., McLoughlin, J.J., Cargill 2nd, R.S.: High rate shear strain of three-dimensional neural cell cultures: a new in vitro traumatic brain injury model. J. Biomech. **38**, 1093–1105 (2005)
18. Edelman, D.B., Keefer, E.W.: A cultural renaissance: in vitro cell biology embraces three-dimensional context. Exp. Neurol. **192**, 1–6 (2005)
19. Cukierman, E., Pankov, R., Stevens, D.R., Yamada, K.M.: Taking cell-matrix adhesions to the third dimension. Science **294**, 1708–1712 (2001)
20. Cukierman, E., Pankov, R., Yamada, K.M.: Cell interactions with three-dimensional matrices. Curr. Opin. Cell. Biol. **14**, 633–639 (2002)
21. Schmeichel, K.L., Bissell, M.J.: Modeling tissue-specific signaling and organ function in three dimensions. J. Cell Sci. **116**, 2377–2388 (2003)
22. Yamada, K.M., Pankov, R., Cukierman, E.: Dimensions and dynamics in integrin function. Braz. J. Med. Biol. Res. **36**, 959–966 (2003)

23. Miller, B.E., Miller, F.R., Heppner, G.H.: Factors affecting growth and drug sensitivity of mouse mammary tumor lines in collagen gel cultures. Cancer Res. **45**, 4200–4205 (1985)
24. Grinnell, F.: Fibroblast biology in three-dimensional collagen matrices. Trends Cell Biol. **13**, 264–269 (2003)
25. Balgude, A.P., Yu, X., Szymanski, A., Bellamkonda, R.V.: Agarose gel stiffness determines rate of DRAG neurite extension in 3M cultures. Biomaterials **22**, 1077–1084 (2001)
26. Coates, P.W., Fermini, B., Strahlendorf, J.C., Strahlendorf, H.K.: Utilization of three-dimensional culture for early morphometric and electrophysiological analyses of solitary cerebellar neurons. Dev. Neurosci. **14**, 35–43 (1992)
27. Coates, P.W., Nathan, R.D.: Feasibility of electrical recordings from unconnected vertebrate CNS neurons cultured in a three-dimensional extracellular matrix. J. Neurosci. Methods **20**, 203–210 (1987)
28. O'Shaughnessy, T.J., Lin, H.J., Ma, W.: Functional synapse formation among rat cortical neurons grown on three-dimensional collagen gels. Neurosci. Lett. **340**, 169–172 (2003)
29. Spector, D.H., Boss, B.D., Strecker, R.E.: A model three-dimensional culture system for mammalian dopaminergic precursor cells: application for functional intracerebral transplantation. Exp. Neurol. **124**, 253–264 (1993)
30. Bellamkonda, R., Ranieri, J.P., Aebischer, P.: Laminin oligopeptide derivatized agarose gels allow three-dimensional neurite extension in vitro. J. Neurosci. Res. **41**, 501–509 (1995)
31. Cullen, D.K., LaPlaca, M.C.: Neuronal response to high rate shear deformation depends on heterogeneity of the local strain field. J. Neurotrauma **23**, 1304–1319 (2006)
32. Cullen, D.K., Lessing, M.C., LaPlaca, M.C.: Collagen-dependent neurite outgrowth and response to dynamic deformation in three-dimensional neuronal cultures. Ann Biomed. Eng. **35**, 835–846 (2007)
33. Vukasinovic, J., Cullen, D.K., LaPlaca, M.C., Glezer, A.: A microperfused incubator for tissue mimetic 3D cultures. Biomed. Microdevices **11**, 1155–1165 (2009)
34. Dillon, G.P., Yu, X., Sridharan, A., Ranieri, J.P., Bellamkonda, R.V.: The influence of physical structure and charge on neurite extension in a 3D hydrogel scaffold. J. Biomater. Sci. Polym. Ed. **9**, 1049–1069 (1998)
35. Willits, R.K., Skornia, S.L.: Effect of collagen gel stiffness on neurite extension. J. Biomater. Sci. Polym. Ed. **15**, 1521–1531 (2004)
36. Schense, J.C., Hubbell, J.A.: Three-dimensional migration of neurites is mediated by adhesion site density and affinity. J. Biol. Chem. **275**, 6813–6818 (2000)
37. Yu, T.T., Shoichet, M.S.: Guided cell adhesion and outgrowth in peptide-modified channels for neural tissue engineering. Biomaterials **26**, 1507–1514 (2005)
38. Yu, X., Bellamkonda, R.V.: Dorsal root ganglia neurite extension is inhibited by mechanical and chondroitin sulfate-rich interfaces. J. Neurosci. Res. **66**, 303–310 (2001)
39. Borkenhagen, M., Clemence, J.F., Sigrist, H., Aebischer, P.: Three-dimensional extracellular matrix engineering in the nervous system. J. Biomed. Mater. Res. **40**, 392–400 (1998)
40. Tsacopoulos, M.: Metabolic signaling between neurons and glial cells: a short review. J. Physiol. Paris **96**, 283–288 (2002)
41. Tsacopoulos, M., Magistretti, P.J.: Metabolic coupling between glia and neurons. J. Neurosci. **16**, 877–885 (1996)
42. Aschner, M.: Neuron-astrocyte interactions: implications for cellular energetics and antioxidant levels. Neurotoxicology **21**, 1101–1107 (2000)
43. Pardo, B., Honegger, P.: Differentiation of rat striatal embryonic stem cells in vitro: monolayer culture vs three-dimensional coculture with differentiated brain cells. J. Neurosci. Res. **59**, 504–512 (2000)
44. Pulliam, L., Stubblebine, M., Hyun, W.: Quantification of neurotoxicity and identification of cellular subsets in a three-dimensional brain model. Cytometry **32**, 66–69 (1998)
45. Irons, H.R., Cullen, D.K., Shapiro, N.P., Lambert, N.A., Lee, R.H., LaPlaca, M.C.: Three-dimensional neural constructs: a novel platform for neurophysiological investigation. J. Neural. Eng. **5**, 333–341 (2008)

46. Ahmed, S.M., Rzigalinski, B.A., Willoughby, K.A., Sitterding, H.A., Ellis, E.F.: Stretch-induced injury alters mitochondrial membrane potential and cellular ATP in cultured astrocytes and neurons. J. Neurochem. **74**, 1951–1960 (2000)
47. Steinschneider, R., Delmas, P., Nedelec, J., Gola, M., Bernard, D., Boucraut, J.: Appearance of neurofilament subunit epitopes correlates with electrophysiological maturation in cortical embryonic neurons cocultured with mature astrocytes. Brain. Res. Dev. Brain. Res. **95**, 15–27 (1996)
48. Nakanishi, K., Nakanishi, M., Kukita, F.: Dual intracellular recording of neocortical neurons in a neuron-glia co-culture system. Brain Res. Brain. Res. Protoc. **4**, 105–114 (1999)
49. LaPlaca, M.C., Vernekar, V.N., Shoemaker, J.T., Cullen, D.K.: Three-dimensional neuronal cultures. In: Berthiaume, F., Morgan, J. (eds.) Methods in Bioengineering: 3D Tissue Engineering. Artech House Publishers, London (2010)
50. Nicholson, C., Sykova, E.: Extracellular space structure revealed by diffusion analysis. Trends Neurosci. **21**, 207–215 (1998)
51. Cullen, D.K., Vukasinovic, J., Glezer, A., Laplaca, M.C.: Microfluidic engineered high cell density three-dimensional neural cultures. J. Neural Eng. **4**, 159–172 (2007)
52. Braitenberg, V.: Brain size and number of neurons: an exercise in synthetic neuroanatomy. J. Comput. Neurosci. **10**, 71–77 (2001)
53. Gabbott, P.L., Stewart, M.G.: Distribution of neurons and glia in the visual cortex (area 17) of the adult albino rat: a quantitative description. Neuroscience **21**, 833–845 (1987)
54. Alves, P., Moreira, J., Rodrigues, J., Aunins, J., Carrondo, M.: Two-dimensional versus three-dimensional culture systems: effects on growth and productivity of BHK cells. Biotechnol. Bioeng. **52**, 429–432 (1996)
55. Kleinman, H.K., McGarvey, M.L., Hassell, J.R., Star, V.L., Cannon, F.B., et al.: Basement membrane complexes with biological activity. Biochemistry **25**, 312–318 (1986)
56. Vukicevic, S., Kleinman, H.K., Luyten, F.P., Roberts, A.B., Roche, N.S., Reddi, A.H.: Identification of multiple active growth factors in basement membrane Matrigel suggests caution in interpretation of cellular activity related to extracellular matrix components. Exp. Cell Res. **202**, 1–8 (1992)
57. Morrison III, B., Cater, H.L., Benham, C.D., Sundstrom, L.E.: An in vitro model of traumatic brain injury utilising two-dimensional stretch of organotypic hippocampal slice cultures. J. Neurosci. Meth. **150**, 192–201 (2006)
58. Stoppini, L., Buchs, P.A., Muller, D.: Lesion-induced neurite sprouting and synapse formation in hippocampal organotypic cultures. Neuroscience **57**, 985–994 (1993)
59. Gahwiler, B.H.: Organotypic monolayer cultures of nervous tissue. J. Neurosci. Meth. **4**, 329–342 (1981)
60. Elkin, B.S., Morrison III, B.: Region-specific tolerance criteria for the living brain. Stapp Car Crash J. **51**, 127–138 (2007)
61. Sieg, F., Wahle, P., Pape, H.C.: Cellular reactivity to mechanical axonal injury in an organotypic in vitro model of neurotrauma. J. Neurotrauma **16**, 1197–1213 (1999)
62. Morrison III, B., Eberwine, J.H., Meaney, D.F., McIntosh, T.K.: Traumatic injury induces differential expression of cell death genes in organotypic brain slice cultures determined by complementary DNA array hybridization. Neuroscience **96**, 131–139 (2000)
63. Krassioukov, A.V., Ackery, A., Schwartz, G., Adamchik, Y., Liu, Y., Fehlings, M.G.: An in vitro model of neurotrauma in organotypic spinal cord cultures from adult mice. Brain Res. Brain Res. Protoc. **10**, 60–68 (2002)
64. Stavridis, S.I., Dehghani, F., Korf, H.W., Hailer, N.P.: Characterisation of transverse slice culture preparations of postnatal rat spinal cord: preservation of defined neuronal populations. Histochem. Cell Biol. **123**, 377–392 (2005)
65. Gahwiler, B.H.: Development of the hippocampus in vitro: cell types, synapses, and receptors. Neuroscience **11**, 751–760 (1984)
66. Del. Rio., J.A., Heimrich, B., Soriano, E., Schwegler, H., Frotscher, M.: Proliferation and differentiation of glial fibrillary acidic protein immunoreactive glial cells in organotypic slice cultures of rat hippocampus. Neuroscience **43**, 335–347 (1991)

67. Caeser, M., Aertsen, A.: Morphological organization of rat hippocampal slice cultures. J. Comp. Neurol. **307**, 87–106 (1991)
68. Stoppini, L., Buchs, P.A., Muller, D.: A simple method for organotypic cultutres of nervous tissue. J. Neurosci. Meth. **37**, 173–182 (1991)
69. Buchs, P.A., Stoppini, L., Muller, D.: Structural modifications associated with synaptic development in area CA1 of rat hippocampal organotypic cultures. Brain Res. Dev. Brain Res. **71**, 81–91 (1993)
70. Mielke, J.G., Comas, T., Woulfe, J., Monette, R., Chakravarthy, B., Mealing, G.A.: Cytoskeletal, synaptic, and nuclear protein changes associated with rat interface organotypic hippocampal slice culture development. Brain Res. Dev. Brain Res. **160**, 275–286 (2005)
71. De Simoni, A., Griesinger, C.B., Edwards, F.A.: Development of rat CA1 neurones in acute versus organotypic slices: role of experience in synaptic morphology and activity. J. Physiol. **550**, 135–147 (2003)
72. Collin, C., Miyaguchi, K., Segal, M.: Dendritic spine density and LTP induction in cultured hippocampal slices. J. Neurophysiol. **77**, 1614–1623 (1997)
73. Gahwiler, B.H.: Slice cultures of cerebellar, hippocampal, and hypothalamic tissue. Experientia **40**, 235–243 (1984)
74. Robain, O., Barbin, G., de Billette, V., Jardin, L., Jahchan, T., Ben-Ari, Y.: Development of mossy fiber synapses in hippocampal slice culture. Brain Res. Dev. Brain Res. **80**, 244–250 (1994)
75. Hartel, R., Matus, A.: Cytoskeletal maturation in cultured hippocampal slices. Neuroscience **78**, 1–5 (1997)
76. Bahr, B.A., Kessler, M., Rivera, S., Vanderklish, P.W., Hall, R.A., et al.: Stable maintenance of glutamate receptors and other synaptic components in long-term hippocampal slices. Hippocampus **5**, 425–439 (1995)
77. Martens, U., Wree, A.: Distribution of [3H]MK-801, [3H]AMPA and [3H]kainate binding sites in rat hippocampal long-term slice cultures isolated from external afferents. Anat. Embryol. (Berl) **203**, 491–500 (2001)
78. Morrison III, B., Pringle, A.K., McManus, T., Ellard, J., Bradley, M., et al.: L-Arginyl-3, 4-Spermidine is neuroprotective in several in vitro models of neurodegeneration and in vivo ischaemia without suppressing synaptic transmission. Brit. J. Pharm. **137**, 1255–1268 (2002)
79. Vornov, J.J., Tasker, R.C., Lost, D.: Direct observation of the agonist-specific regional vulnerability to glutamate, NMDA, and kainate neurotoxicity in organotypic hippocampal cultures. Exp. Neurol. **114**, 11–22 (1991)
80. Gutierrez, R., Heinemann, U.: Synaptic reorganization in explanted cultures of rat hippocampus. Brain Res. **815**, 304–316 (1999)
81. Parent, J.M., Yu, T.W., Leibowitz, R.T., Geschwind, D.H., Sloviter, R.S., Lowenstein, D.H.: Dentate granule cell neurogenesis is increased by seizures and contributes to aberrant network reorganization in the adult rat hippocampus. J. Neurosc. Off. J. Soc. Neurosci. **17**, 3727–3738 (1997)
82. Muller, D., Buchs, P.A., Stoppini, L.: Time course of synaptic development in hippocampal organotypic cultures. Brain Res. Mol. Brain Res. **71**, 93–100 (1993)
83. McBain, C.J., Boden, P., Hill, R.G.: Rat hippocampal slices 'in vitro' display spontaneous epileptiform activity following long-term organotypic culture. J. Neurosci. Meth. **27**, 35–49 (1989)
84. Fowler, J., Bornstein, M.B., Crain, S.M.: Sustained hyperexcitability elicited by repetitive electric stimulation of organotypic hippocampal explants. Brain Res. **378**, 398–404 (1986)
85. Xiang, Z., Hrabetova, S., Moskowitz, S.I., Casaccia-Bonnefil, P., Young, S.R., et al.: Long-term maintenance of mature hippocampal slices in vitro. J. Neurosci. Meth. **98**, 145–154 (2000)
86. Finley, M., Fairman, D., Liu, D., Li, P., Wood, A., Cho, S.: Functional validation of adult hippocampal organotypic cultures as an in vitro model of brain injury. Brain Res. **1001**, 125–132 (2004)

87. Wilhelmi, E., Schoder, U.H., Benabdallah, A., Sieg, F., Breder, J., Reymann, K.G.: Organotypic brain-slice cultures from adult rats: approaches for a prolonged culture time. Altern. Lab Anim. **30**, 275–283 (2002)
88. Takhounts, E.G., Eppinger, R.H., Campbell, J.Q., Tannous, R.E., Power, E.D.: On the development of the SIMon finite element head model. Stapp Car Crash J. **47**, 107–133 (2003)
89. Cheng, S., Clarke, E.C., Bilston, L.E.: Rheological properties of the tissues of the central nervous system: a review. Med. Eng. Phys. **30**, 1318–1337 (2008)
90. Hrapko, M., van Dommelen, J.A., Peters, G.W., Wismans, J.S.: The influence of test conditions on characterization of the mechanical properties of brain tissue. J. Biomech. Eng. **130**, 031003 (2008)
91. Fallenstein, G.T., Hulce, V.D.: Dynamic mechanical properties of human brain tissue. J. Biomech. **2**, 217–226 (1969)
92. Arbogast, K.B., Margulies, S.S.: Material characterization of the brainstem from oscillatory shear tests. J. Biomech. **31**, 801–807 (1998)
93. Nicolle, S., Lounis, M., Willinger, R., Palierne, J.F.: Shear linear behavior of brain tissue over a large frequency range. Biorheology **42**, 209–223 (2005)
94. Bilston, L.E., Liu, Z., Phan-Thien, N.: Large strain behaviour of brain tissue in shear: some experimental data and differential constitutive model. Biorheology **38**, 335–345 (2001)
95. Takhounts E., Crandall, J.R., Darvish, K.K.: On the importance of nonlinearity of brain tissue under large deformations. Stapp Car Crash J. **47**, 79–92 (2003)
96. Tamura, A., Hayashi, S., Watanabe, I., Nagayama, K., Matsumoto, T.: Mechanical characterization of brain tissue in high-rate compression. J. Biomech. Sci. Eng. **2**, 115–126 (2007)
97. Cheng, S., Bilston, L.E.: Unconfined compression of white matter. J. Biomech. **40**, 117–124 (2007)
98. Miller, K., Chinzei, K.: Mechanical properties of brain tissue in tension. J. Biomech. **35**, 483–490 (2002)
99. Franceschini, G., Bigoni, D., Regitnig, P., Holzapfel, G.A.: Brain tissue deforms similarly to filled elastomers and follows consolidation theory. J. Mech. Phys. Solids **54**, 2592–2620 (2006)
100. Mao, H., Jin, X., Zhang, L., Yang, K.H., Igarashi, T., et al.: Finite element analysis of controlled cortical impact-induced cell loss. J. Neurotrauma **27**, 877–888 (2010)
101. Hicks, R., Soares, H., Smith, D., McIntosh, T.: Temporal and spatial characterization of neuronal injury following lateral fluid-percussion brain injury in the rat. Acta Neuropathol. **91**, 236–246 (1996)
102. van Dommelen, J.A., van der Sande, T.P., Hrapko, M., Peters, G.W.: Mechanical properties of brain tissue by indentation: interregional variation. J. Mech. Behav. Biomed. Mater. **3,** 158–166 (2010)
103. Gefen, A., Margulies, S.S.: Are in vivo and in situ brain tissues mechanically similar? J. Biomech. **37**, 1339–1352 (2004)
104. Elkin, B.S., Azeloglu, E.U., Costa, K.D., Morrison III, B.: Mechanical heterogeneity of the rat hippocampus measured by AFM indentation. J. Neurotrauma **24**, 812–822 (2007)
105. Elkin, B.S., Ilankovan, A., Morrison, III B.: Age-dependent regional mechanical properties of the rat hippocampus and cortex. J. Biomech. Eng. **132**, 011010 (2010)
106. Elkin, B.S., Ilankovan, A., Morrison, III B.: A detailed viscoelastic characterization of the P17 and adult rat brain. J. Neurotrauma (2011, in press)
107. Tripathy, S., Berger, E.J.: Measuring viscoelasticity of soft samples using atomic force microscopy. J. Biomech. Eng. **131**, 094507 (2009)
108. Neubert, H.K.P.: A simple model representing internal damping in solid materials. Aeronaut. Quart. **14**, 187–210 (1963)
109. Schiessel, H., Metzler, R., Blumen, A., Nonnenmacher, T.F.: Generalized viscoelastic models: their fractional equations with solutions. J. Phys. A Math. Gen. **28**, 6567–6584 (1995)

110. Harding, J.W., Sneddon, I.N.: The elastic stresses produced by the indentation of the plane surface of a semi-infinite elastic solid by a rigid punch. Proc. Camb. Philol. Soc. **41**, 16–26 (1945)
111. Cheng, L., Xia, X., Yu, W., Scriven, L.E., Gerberich, W.W.: Flat-punch indentaiton of viscoelastic material. J. Polym. Sci. B **38**, 10–22 (2000)
112. Hayes, W.C., Keer, L.M., Herrmann, G., Mockros, L.F.: A mathematical analysis for indentation tests of articular cartilage. J. Biomech. **5**, 541–551 (1972)
113. Lu, Y.B., Franze, K., Seifert, G., Steinhauser, C., Kirchhoff, F., et al.: Viscoelastic properties of individual glial cells and neurons in the CNS. Proc. Natl. Acad. Sci. U.S.A **103**, 17759–17764 (2006)
114. Darvish, K.K., Crandall, J.R.: Nonlinear viscoelastic effects in oscillatory shear deformation of brain tissue. Med. Eng. Phys. **23**, 633–645 (2001)
115. Donnelly, B.R., Medige, J.: Shear properties of human brain tissue. J. Biomech. Eng. **119**, 423–432 (1997)
116. Rivlin, R.S.: Large elastic deformations of isotropic material I fundamental concepts. Philol. Trans. R. Soc. Lond. A **240**, 459–490 (1948)
117. Mooney, M.: A theory of large elastic deformation. J. Appl. Phys. **11**, 582–592 (1940)
118. Adkins, J.E., Rivlin, R.S.: Large elastic deformations of isotropic materials IX. The deformation of thin shells. Philol. Trans. R. Soc. Lond. A **244**, 505–531 (1952)
119. Ogden, R.W.: Large deformation isotropic elasticity—correlation of theory and experiment for compressible rubberlike solids. Proc. R. Soc. Lond. A **328**, 567–583 (1972)
120. Gefen, A., Gefen, N., Zhu, Q., Raghupathi, R., Margulies, S.S.: Age-dependent changes in material properties of the brain and braincase of the rat. J. Neurotrauma **20**, 1163–1177 (2003)
121. Prange, M.T., Margulies, S.S.: Regional, directional, and age-dependent properties of the brain undergoing large deformation. J. Biomech. Eng. **124**, 244–252 (2002)
122. Ting, T.C.T.: Contact stresses between a rigid indenter and a viscoelastic half-space. J. Appl. Mech. **33**, 845–854 (1966)
123. Segedin, C.M.: The relationship between load and penetration for a spherical punch. Mathematika **4**, 156–161 (1957)
124. Sneddon, I.N.: The relation between load and penetration in the axisymmetric Boussinesq problem for a punch of arbitrary profile. Int. J. Eng. Sci. **3**, 47–57 (1965)
125. Mahaffy, R.E., Park, S., Gerde, E., Kas, J., Shih, C.K.: Quantitative analysis of the viscoelastic properties of thin regions of fibroblasts using atomic force microscopy. Biophys. J. **86**, 1777–1793 (2004)
126. Mahaffy, R.E., Shih, C.K., MacKintosh, F.C., Kas, J.: Scanning probe-based frequency-dependent microrheology of polymer gels and biological cells. Phys. Rev. Lett. **85**, 880–883 (2000)
127. Alcaraz, J., Buscemi, L., Puig-de-Morales, M., Colchero, J., Baro, A., Navajas, D.: Correction of microrheological measurements of soft samples with atomic force microscopy for the hydrodynamic drag on the cantilever. Langmuir **18**, 716–721 (2002)
128. Lodge AS. 1964. *Elastic Liquids*. London: Academic Press
129. Wilhelm, M.: Fourier-transform rheology. Macromol. Mater. Eng. **287**, 83–105 (2002)
130. Cho, K.S., Hyun, K., Ahn, K.H., Lee, S.J.: A geometrical interpretation of large amplitude oscillatory shear response. J. Rheol. **49**, 747–758 (2005)
131. Ewoldt, R.H., Hosoi, A.E., McKinley, G.H.: New measures for characterizing nonlinear viscoelasticity in large amplitude oscillatory shear. J. Rheol. **52**, 1427–1458 (2008)
132. Coats, B., Margulies, S.S.: Material properties of porcine parietal cortex. J. Biomech. **39**, 2521–2525 (2006)
133. Thibault, K.L., Margulies, S.S.: Age-dependent material properties of the porcine cerebrum: effect on pediatric inertial head injury criteria. J. Biomech. **31**, 1119–1126 (1998)
134. Gillespie, P.G., Muller, U.: Mechanotransduction by hair cells: models, molecules, and mechanisms. Cell **139**, 33–44 (2009)

135. Lin, Y.W., Cheng, C.M., Leduc, P.R., Chen, C.C.: Understanding sensory nerve mechanotransduction through localized elastomeric matrix control. PLoS One **4**, e4293 (2009)
136. Stabenfeldt, S.E., Garcia, A.J., LaPlaca, M.C.: Thermoreversible laminin-functionalized hydrogel for neural tissue engineering. J. Biomed. Mater. Res. A **77A**, 718–725 (2006)
137. Dai, W.G., Belt, J., Saltzman, W.M.: Cell-binding peptides conjugated to poly(ethylene glycol) promote neural cell-aggregation. Bio-Technology **12**, 797–801 (1994)
138. Hern, D.L., Hubbell, J.A.: Incorporation of adhesion peptides into nonadhesive hydrogels useful for tissue resurfacing. J. Biomed. Mater. Res. **39**, 266–276 (1998)
139. Mahoney, M.J., Anseth, K.S.: Three-dimensional growth and function of neural tissue in degradable polyethylene glycol hydrogels. Biomaterials **27**, 2265–2274 (2006)
140. Georges, P.C., Miller, W.J., Meaney, D.F., Sawyer, E.S., Janmey, P.A.: Matrices with compliance comparable to that of brain tissue select neuronal over glial growth in mixed cortical cultures. Biophys. J. **90**, 3012–3018 (2006)
141. Flanagan, L.A., Ju, Y.E., Marg, B., Osterfield, M., Janmey, P.A.: Neurite branching on deformable substrates. Neuroreport **13**, 2411–2415 (2002)
142. Guo, W.H., Frey, M.T., Burnham, N.A., Wang, Y.L.: Substrate rigidity regulates the formation and maintenance of tissues. Biophys. J. **90**, 2213–2220 (2006)
143. Pelham Jr., R.J., Wang, Y.: Cell locomotion and focal adhesions are regulated by substrate flexibility. Proc. Natl. Acad. Sci. U.S.A. **94**, 13661–13665 (1997)
144. Engler, A.J., Griffin, M.A., Sen, S., Bonnemann, C.G., Sweeney, H.L., Discher, D.E.: Myotubes differentiate optimally on substrates with tissue-like stiffness: pathological implications for soft or stiff microenvironments. J. Cell. Biol. **166**, 877–887 (2004)
145. Georges, P.C., Janmey, P.A.: Cell type-specific response to growth on soft materials. J. Appl. Physiol. **98**, 1547–1553 (2005)
146. Slemmer, J.E., Matser, E.J., de Zeeuw, C.I., Weber, J.T.: Repeated mild injury causes cumulative damage to hippocampal cells. Brain **125**, 2699–2709 (2002)
147. Balentine, J.D., Greene, W.B., Bornstein, M.: In vitro spinal cord trauma. Lab. Invest. **58**, 93–99 (1988)
148. Regan, R.F., Choi, D.W.: The effect of NMDA, AMPA/kainate, and calcium channel antagonists on traumatic cortical neuronal injury in culture. Brain Res. **633**, 236–242 (1994)
149. Cargill, R.S., Thibault, L.E.: Acute alterations in [Ca2 +]i in NG108–15 cells subjected to high strain rate deformation and chemical hypoxia: An in vitro model for neural trauma. J. Neurotrauma **13**, 395–407 (1996)
150. Ellis, E.F., McKinney, J.S., Willoughby, K.A., Liang, S., Povlishock, J.T.: A new model for rapid stretch-induced injury of cells in culture: Characterization of the model using astrocytes. J. Neurotrauma **12**, 325–339 (1995)
151. LaPlaca, M.C., Thibault, L.E.: An in vitro traumatic injury model to examine the response of neurons to a hydrodynamicaly induced deformation. Ann. Biomed. Eng. **25**, 665–677 (1997)
152. Morrison III, B., Meaney, D.F., McIntosh, T.K.: Mechanical characterization of an in vitro device designed to quantitatively injure living brain tissue. Ann. Biomed. Eng. **26**, 381–390 (1998)
153. Smith, D.H., Wolf, J.A., Lusardi, T.A., Lee, V.M., Meaney, D.F.: High tolerance and delayed elastic response of cultured axons to dynamic stretch injury. J. Neurosci. **19**, 4263–4269 (1999)
154. Morrison III, B., Cater, H.L., Wang, C.C., Thomas, F.C., Hung, C.T., et al.: A tissue level tolerance criterion for living brain developed with an in vitro model of traumatic mechanical loading. Stapp Car Crash J. **47**, 93–105 (2003)
155. Elkin, B.S., Morrison 3rd, B.: Region-specific tolerance criteria for the living brain. Stapp Car Crash J. **51**, 127–138 (2007)
156. LaPlaca, M.C., Lee, V.M., Thibault, L.E.: An in vitro model of traumatic neuronal injury: loading rate-dependent changes in acute cytosolic calcium and lactate dehydrogenase release. J. Neurotrauma **14**, 355–368 (1997)

157. Geddes, D.M., Cargill 2nd, R.S., LaPlaca, M.C.: Mechanical stretch to neurons results in a strain rate and magnitude-dependent increase in plasma membrane permeability. J. Neurotrauma **20**, 1039–1049 (2003)
158. Pfister, B.J., Weihs, T.P., Betenbaugh, M., Bao, G.: An in vitro uniaxial stretch model for axonal injury. Ann. Biomed. Eng. **31**, 589–598 (2003)
159. Lusardi, T.A., Rangan, J., Sun, D., Smith, D.H., Meaney, D.F.: A device to study the initiation and propagation of calcium transients in cultured neurons after mechanical stretch. Ann. Biomed. Eng. **32**, 1546–1558 (2004)
160. Cater, H.L., Sundstrom, L.E., Morrison III, B.: Temporal development of hippocampal cell death is dependent on tissue strain but not strain rate. J. Biomech. **39**, 2810–2818 (2006)
161. Bain, A.C., Meaney, D.F.: Tissue-level thresholds for axonal damage in an experimental model of central nervous system white matter injury. J. Biomech. Eng. **122**, 615–622 (2000)
162. Galle, B., Ouyang, H., Shi, R., Nauman, E.: Correlations between tissue-level stresses and strains and cellular damage within the guinea pig spinal cord white matter. J. Biomech. **40**, 3029–3033 (2007)
163. Barbee, K.A.: Mechanical cell injury. Ann. N. Y. Acad. Sci. **1066**, 67–84 (2005)
164. Kumaria, A., Tolias, C.M.: In vitro models of neurotrauma. Br. J. Neurosurg **22**, 200–206 (2008)
165. LaPlaca, M.C., Simon, C.M., Prado, G.R., Cullen, D.K.: CNS injury biomechanics and experimental models. Prog. Brain Res. **161**, 13–26 (2007)
166. Morrison III, B., Saatman, K.E., Meaney, D.F., McIntosh, T.K.: In vitro central nervous system models of mechanically induced trauma: a review. J. Neurotrauma **15**, 911–928 (1998)
167. Geddes, D.M., LaPlaca, M.C., Cargill, R.S.: Susceptibility of hippocampal neurons to mechanically induced injury. Exp. Neurol. **184**, 420–427 (2003)
168. Lusardi, T.A., Wolf, J.A., Putt, M.E., Smith, D.H., Meaney, D.F.: Effect of acute calcium influx after mechanical stretch injury in vitro on the viability of hippocampal neurons. J. Neurotrauma **21**, 61–72 (2004)
169. Lusardi, T.A., Smith, D.H., Wolf, J.A., Meaney, D.F.: The separate roles of calcium and mechanical forces in mediating cell death in mechanically injured neurons. Biorheology **40**, 401–409 (2003)
170. DeRidder, M.N., Simon, M.J., Siman, R., Auberson, Y.P., Raghupathi, R., Meaney, D.F.: Traumatic mechanical injury to the hippocampus in vitro causes regional caspase-3 and calpain activation that is influenced by NMDA receptor subunit composition. Neurobiol. Dis. **22**, 165–176 (2006)
171. Geddes-Klein, D.M., Schiffman, K.B., Meaney, D.F.: Mechanisms and consequences of neuronal stretch injury in vitro differ with the model of trauma. J. Neurotrauma **23**, 193–204 (2006)
172. Yu, Z., Morrison III, B.: Experimental mild traumatic brain injury induces functional alteration of the developing hippocampus. J. Neurophysiol. **103**, 499–510 (2010)
173. Prado, G.R., Ross, J.D., Deweerth, S.P., LaPlaca, M.C.: Mechanical trauma induces immediate changes in neuronal network activity. J. Neural. Eng. **2**, 148–158 (2005)